Merimon 2001 - Final Report

van der Woerd, H.J.; Eleveld, M.A.; Hakvoort, H.; Pasterkamp, R.; Peters, S.W.M.

2003

document version
Publisher's PDF, also known as Version of record

MERIMON 2001

Final Report

H.J. van der Woerd, M. Eleveld, H. Hakvoort, R. Pasterkamp & S.W.M. Peters

E-03/04

June 19, 2003

IVM acknowledges dr.ir. J.E. Vermaat for refereeing this report

IVM

Institute for Environmental Studies
Vrije Universiteit
De Boelelaan 1087
1081 HV Amsterdam
The Netherlands

Tel. ++31-20-4449 555
Fax. ++31-20-4449 553
E-mail: info@ivm.falw.vu.nl

Contents

Abstract iii

Samenvatting v

Glossary of Symbols and acronyms vii

1. Introduction 1
   1.1 Scope 1
   1.2 Goal 1
   1.3 MERIMON First Results 2
   1.4 Set-up of the project and this report 3
   1.5 Acknowledgement 4

2. A sensitivity analysis of analytical inversion methods to derive chlorophyll from MERIS spectra in case-II waters 5
   Abstract 5
   2.1 Basics of forward and inverse modelling: The Gordon model and the SIOP model 5
   2.2 Set-up of the sensitivity analysis 6
   2.3 Types of Analytical algorithms tested 6
   2.4 Hybrid Iterative Inversion Methods (*HIM*) 7
   2.5 Initial estimations of TCHL, TSM and CDOM 7
      2.5.1 Initial CHL 7
      2.5.2 Initial CDOM 8
      2.5.3 Initial TSM 8
   2.6 In-situ measurements 9
      2.6.1 (S)IOP measurement methods 9
   2.7 MERIS band settings 9
   2.8 results and discussion 9

3. Results from MERIS rehearsal 15
   3.1 Radiometric calibration of the PR-650 15
   3.2 Field campaign results 16
   3.3 Comparison IVM3 vs. L4_15_A 18
   3.4 Comparison MA_16 vs. IVM13 20
   3.5 Comparison L4_16 vs. IVM19 21
   3.6 Summary and recommendations 22

4. MERIS validation of geophysical ocean colour products: preliminary results for the Netherlands 23
   Abstract 23
   4.1 Introduction 23
   4.2 Methodology 24

4.2.1 Cruise planning 24
4.2.2 Protocols 24
4.2.3 Used software & tools 26
4.3 Available Imagery 26
4.4 Results 27
4.4.1 Concentrations 28
4.4.2 Reflectance 28
4.5 Conclusions and Recommendations 30
4.6 Tables 31

5. Processed MERIS and CASI observations 35
5.1 Processing of a MERIS image with regional algorithms 35
5.2 Processing of CASI imagery 38
5.2.2 Masking 40
5.2.3 Results 41

References 43

Appendix I. MERIS prototype processing infrastructure 45

Appendix II. Implementation of the used algorithms in ERDAS imagine 49

Abstract

This report describes the results of the MERIMON study in the years 2001 and 2002. The MERIMON project was set up in the year 2000 to prepare the operational use of validated MERIS products by establishing the science and software to handle and analyse MERIS observations in combination with in-situ measurements.

The MERIS instrument (Medium Resolution Imaging Spectrometer) was build by ESA and launched on the ENVISAT platform on March 1st 2002. Before the launch two workshops were organized to define the protocols for in-situ measurements and establish inter-comparison measurements of in-situ under-water measurements, laboratory analysis and above water reflectance measurements. The IVM measurements with PR650 comply with the protocols and standards and turn out to be important in the validation of the MERIS level-2 product R(0-).

After the ENVISAT launch a campaign was undertaken to collect so-called match-up data. In collaboration with the RIKZ/DNZ Mitra vessel, in-situ measurements were made in the Dutch coastal waters close to the time of MERIS overpass. In addition much effort was put in the collection of airborne remote sensing observations of these waters by the EPS-A scanner and CASI Imaging spectrometer. In the summer of 2002 a number of good and reliable observations were made and combined with MERIS data. The results show that MERIS operates well from a technical point of view. The results also indicate the need for a regional processor and regional algorithms to properly derive estimates for the water quality parameters CHL, TSM and CDOM.

Samenvatting

Voor u ligt het rapport met de resultaten van het MERIMON project, behaald in 2001 en 2002. Het MERIMON project begon in het jaar 2000 en had tot doel de validatie van MERIS waterkwaliteit producten voor te bereiden en uit te voeren in de Nederlandse wateren. Dit gebeurde door de collectie van *in-situ* metingen, het ontwikkelen van algoritmen en het ontwikkelen van software.

Het MERIS instrument (Medium Resolution Imaging Spectrometer) is ontwikkeld door ESA en werd gelanceerd op ENVISAT op 1 maart 2002. Ter voorbereiding van de validatie, voor de lancering, heeft het IVM deelgenomen aan twee workshops. Op deze workshops zijn afspraken gemaakt over metingen en meetprotocollen, zijn vergelijkende meetcampagnes uitgevoerd om verschillende instrumenten te intercalibreren en zijn laboratorium metingen getoetst. De metingen met de PR650 spectrofotometer van de boven-water reflectantie blijkt een betrouwbare en succesvolle validatie meting van het MERIS R(0-) product.

Na de lancering van ENVISAT is in 2002 een campagne uitgevoerd om in-situ en reflectie metingen te verzamelen ten tijde van een MERIS waarneming. Dit gebeurde aan boord van het RIKZ/DNZ Mitra schip op raaien die standaard in de Nederlandse kustzone worden gevaren. Bij de internationale validatie bijeenkomst in Frascati (december 2002) bleek dat dit heeft geleid tot 2 van de 8 betrouwbare validatiemetingen in troebele kustwateren.

In 2002, net als in het jaar ervoor is bijzonder veel moeite gedaan om vanuit een vliegtuig additionele spectrale beeldende metingen te krijgen. Met de EPS-A is dit niet gelukt. In september zijn wel, in opdracht van de MD, met een CASI instrument extra metingen gedaan. Deze metingen worden geïnterpreteerd en vergeleken met het MERIS beeld rondom die opname.

Samenvattend heeft dit project geleid tot kennis en infrastructuur om MERIS beelden van de Nederlandse wateren te behandelen en de kwaliteit te beoordelen. MERIS blijkt technisch goed te werken. De voor u liggende analyses benadrukken ook dat er behoefte blijft om voor de Nederlandse wateren toegesneden producten te maken naast standaard ESA producten.

Glossary of Symbols and acronyms

Symbol	Description	Units
TCHL	Concentration of Chlorophyll-a and phaeopigments	mg m^{-3}
TSM	Concentration of total suspended matter	g m^{-3}
CDOM	Concentration of Coloured Dissolved Organic Matter (expressed as absorption at 440nm)	m^{-1}
CHL	Concentration of chlorophyll a	mg m^{-3}
IOP	Inherent Optical Properties	
SIOP	Specific Inherent Optical properties	
A	Total absorption coefficient	m^{-1}
a_{CDOM}	Absorption coefficient of CDOM	m^{-1}
a_w	Absorption coefficient of pure water	m^{-1}
$\bar{a}_{CDOM}$	Absorption coefficient of CDOM, normalised at 440nm	-
a^*_{CHL}	Specific absorption coefficient of CHL	m^2 mg^{-1}
a^*_{TSM}	Specific absorption coefficient of TSM	m^2 g^{-1}
G_{440}	Absorption by CDOM at 440 nm	m^{-1}
B	Total scattering coefficient	m^{-1}
b_b	Total back scattering coefficient (scattering for angles > 90° with respect to direction of incoming light)	m^{-1}
b_w	scattering coefficient of pure water	m^{-1}
$b^*_{b,TSM}$	specific back scattering coefficient of TSM	m^2 g^{-1}
B	Backscatter to scatter ratio	-
λ	Wavelength	Nm
θ_0	Angle of downwelling sun light under water	-
$\mu_{u,d}$	average cosine of upwelling (u) or downwelling (d) light	-
θ_z	Sun zenith angle	-
E_{wd}	subsurface downward irradiance	W m^{-2} nm^{-1}
E_{wu}	subsurface upward irradiance	W m^{-2} nm^{-1}
F	prefactor in Gordon formulae	-
F	fraction diffuse light of downward irradiance	-
L_{wd}	subsurface downward radiance	W m^{-2} sr^{-1} nm^{-1}
L_{wu}	subsurface upward radiance	W m^{-2} sr^{-1} nm^{-1}
Q	conversion coefficient for L_{wu} to E_{wu}	-

R(0-)	subsurface irradiance reflectance	
$R(0^-,\lambda)$	subsurface irradiance reflectance at wavelength λ	-
$R(0^+,\lambda)$	above surface radiance reflectance at wavelength λ	-
EPS-A	Europe Probe Scanner: hyperspectral imaging spectrometer installed on board of the Dutch coast guard aircraft	
MOS	Modular Optoelectronic Scanner	
MERIS	Medium Resolution Imager	
PR650	Photo Research 650 spectroradiometer	
Satlantics	Portable multi-channel spectroradiometer	
SeaWiFS	Sea-viewing Wide Field-of-View Sensor	
PCD	Product Control Data	
Hydrolight	Computer simulation code for underwater light modelling	
DOC	Demonstration Ocean Colour Project	
ENVISAT-AO	Announcenment of Opportunities for Research for calibration/validation of ENVISAT products	
ESA-DUP	Data User Programme of ESA	
MERIMON	MERIS for water quality MONitoring in the Belgian-Dutch-German coastal zone: this study	
PMNS	Particulate Matter North Sea	
POWERS	Pre-Operational Water and Environment Regional Service Project	
ESA	European Space Agency	
IVM	Institute for Environmental Studies	
	Instituut Voor Milieuvraagstukken	
NIOZ	National Institute for Sea Research	
RWS/MD	Rijkswaterstaat Meetkundige Dienst	
	Department of Waterworks, Survey Department	
RIKZ	Rijks Instituut Kust en Zee	
	Department of Waterworks, National Institute for Coastal and Marine Management	
Belgica	Belgian Monitoring vessel	
Mitra	Monitoring vessel of Rijkswaterstaat	
Navicula	Research Vessel of NIOZ	
MAVT	MERIS and AATSR Validation Team	

MIM	Matrix Inversion Method
MRA	Multiple Regression Analysis
NN	Neural Networks
RMI	Ratio Matrix Inversion Method
RS	Remote Sensing

1. Introduction

1.1 Scope

MERIMON constitutes the Dutch contribution to the ENVISAT validation proposal MERSOPS (MERIS region-specific optical properties calibration for water quality monitoring in the Belgian-Dutch-German coastal zone). The MERSOPS proposal was submitted to ESA by MUMM on behalf of the contributing parties MUMM (B), IVM (NL) and GKSS (D). MERIMON is one of the four core validation activities in the ESA MAVT.

The main objective of the MERIMON project is to optimise the calibration of the standard MERIS bio-optical model by assimilating region-specific information relating inherent optical properties to chlorophyll and suspended matter concentrations. MERIMON contributes to this objective through a concentrated effort to collect data for calibration and validation of MERIS algorithms and MERIS products for Dutch coastal waters. ENVISAT was originally scheduled for launch in July 2001. The definite launch took place on March 1st 2002. This had major implications for the workplan, including a shift in the planning of ship time and airborne observations from 2001 to the year 2002. The first MERIS products were delivered to IVM begin of October 2002.

The results of this report build upon earlier projects; in particular we mention the PMNS, POWERS and Demo Ocean Colour projects. MERIMON was started in the year 2000. The results of the first year are extensively described in Peters et al. (2001).

1.2 Goal

The main objective of MERIMON in the years 2001 and 2002 is aimed at producing validated (i.e. of known accuracy) suspended matter maps and chlorophyll concentration maps, based on MERIS observations.

TSM-maps

The DUP-POWERS project (Van der Woerd et al., 1999) and MERIMON-2000 project (Peters et al., 2001) have demonstrated that these products are feasible, even with a satellite as SeaWiFS that is not designed specifically for coastal water research. Therefore MERIMON-2001 aims at producing validated regional TSM products using MERIS observations (in the context of this proposal regional stands for Dutch coastal waters). MERIMON-2000 has shown that regional TSM products should be based on observations of regional inherent optical properties and a validated regional analytical algorithm. The validation of TSM products will require also a validation of MERIS observed water-leaving radiance, which is addressed in this project. When validated MERIS TSM products will become available, they will significantly enhance ongoing operational use of such products (such as the Rijkswaterstaat commissioned TSM atlas of the North Sea)

CHL-maps

These image products will be of increasing importance because the Belgian/Dutch/ German/Danish coastal zone has been defined as a eutrophication problem area (OSPARCOM, 1995). Consequently, these countries are obliged to take steps to reduce nutrient inputs into this area. Additional monitoring of phytoplankton concentration will have to take place. CHL-maps derived from satellite data are a promising new form of information (REVAMP, 2002). MERIMON-2000 has already shown the feasibility of SeaWiFS and MERIS based CHL products, but such products still have to be validated.

1.3 MERIMON First Results

In MERIMON-2000 (Peters et al., 2001) datasets were obtained at two locations at the time of spring algal blooms (Noordwijk and Marsdiep). A third location (Belgian coastal waters) was sampled separately; the research was commissioned by RWS/MD. Distinctly different water types were found at all three locations. The properties of the water at the Noordwijk measurement locations approximately represent the average for North Sea water along the Dutch Belgian coast.

Ship-borne measurements (above water) of seawater surface spectra are generally suitable to validate TSM and CHL concentration retrieval methods, thus validating the use of retrieval algorithms for satellite data. These methods, using the PR650 spectrometer, could be validated using in-situ concentrations. MERIMON-2000 results indicate that this method is very accurate and innovative. Ferry-borne radiometric observations are a helpful instrument for MERIS validation too. The Marsdiep was found to be a very a-typical water type (compared to other North Sea locations). Therefore the site is ideal for checks on ranges in water types that will de detected in the satellite products.

The most accurate methods to obtain CHL and TSM from reflectance spectra are based on analytical algorithms. Two candidate analytical algorithms for regional MERIS products were identified, namely the Matrix Inversion Method (MIM) and the new Ratio Matrix Inversion method (RMI). RMI proved to be the best algorithm for CHL and TSM retrieval from PR650 spectra and SeaWiFS images. MIM produced good results for TSM retrieval. With RMI, a series of SeaWiFS based TSM- and CHL-demonstration products were produced for May 2000.

Analytical algorithms have to be parameterised and calibrated using (averaged sets of) in-situ measured inherent- and apparent- optical properties. In 2000 three sets of measurements were obtained, mostly during the spring phytoplankton bloom. Analytical algorithms calibrated with these parameters are valid for these conditions and possibly also for other conditions as well, but this remains to be tested by sensitivity analysis. This sensitivity analysis requires an insight into the range of variation in inherent and apparent optical properties for the Dutch North Sea. This range is fortunately reasonably well covered by the MERIMON-2000 and PMNS datasets that comprise a large range of TSM (Belgian waters) and CDOM (Marsdiep) values.

Validation of image products derived with regional MERIS algorithms based on EPS-A image products was hampered because of image quality deterioration due to sun-glint. However, this testing and tuning of the algorithms on airborne images is an important

step in the MERIS validation and was included in the year 2002. The EPS-A is a very suitable instrument for coastal applications and an interesting MERIS proxy sensor. The MERIS band settings are very suitable for TSM and CHL concentration retrieval in Dutch coastal waters.

1.4 Set-up of the project and this report

From the lessons learned in the first phase of MERIMON and the goal to make a proper validation of the MERIS products at the end of the year 2002, the following activities were undertaken in the MERIMON-2001 project:

1. Selection of the final regional analytical algorithm.

To select the most reliable algorithm for the derivation of water-quality products in the Dutch coastal waters, a sensitivity study was performed. By means of bio-optical model simulations and model inversion the sensitivity of a range of algorithms was tested. The SIOP values observed in 2000 served as a reference database. The results were presented at the Ocean Optics conference in Santa Fe (2002) and are described in Chapter 2.

2. Rehearsal for the generation of a regional TSM and CHL map.

Before the launch of MERIS the MERIMON team participated in a number of workshops to update measurement protocols, to calibrate and compare instruments and to do a rehearsal of the upload of validation measurements to the MAVT-NILU database. This rehearsal is mandatory for the MAVT activities and took place near Plymouth. The results from the MAVT rehearsals, relevant for MERIMON are reported in Chapter 3.

3. Validation of MERIS standard measurements.

A MERIS prototype-processing infrastructure was developed based on existing software (mainly ESA MATBX tools). MERIS products are not compatible to SeaDAS software or commercially available software such as ENVI/IDL. Additionally, existing prototype software for the regional algorithm (as developed in MERIMON-2000) was adapted for use with actual MERIS images. This is described in Appendix I.

MERIMON is one of the projects to validate MERIS products in co-operation with the ESA/MAVT (MERIS and AATSR Validation Team). Multiple TSM and CHL measurements at representative sites, accompanied by observations of water leaving radiance spectra, to validate MERIS observations and standard products during the commissioning phase have been performed. The validation was reported at the ESA validation and calibration meeting in Frascati; see Chapter 4.

4. Production of regional TSM maps and comparison with airborne data.

Early September, a CASI overflight took place near the mouth of the Western Scheldt estuary. The band setting was almost identical to the MERIS band setting. In chapter 5 we report on the analysis of these CASI images. The processing in ERDAS 8.5 is reported in Appendix II. A low-resolution observation by MERIS, one day later was analysed and processed to CHL and TSM maps, based on local SIOP-fed algorithms.

1.5 Acknowledgement

This research was sponsored by the BCRS and NIVR under number GO-2 2.3/AP-08. We thank Ad van Mullen and Sylvian de Valk from AquaSense for the sampling and determination of inherent optical properties and concentrations and the IVM-Lab (Gerda Hopman-Ubbels) for the reflectance measurements. We are very appreciative for the opportunity to join the monitoring cruises of the M/S Mitra and we would like to thank the staff, captain and crew of the M/S Mitra for their flexibility and kindness. Drs. G.J. van den Berg from the MD supported the processing and delivery of CASI images. Finally we thank the ESA, ACRI and Brockmann Consult for the delivery of MERIS imagery.

2. A sensitivity analysis of analytical inversion methods to derive chlorophyll from MERIS spectra in case-II waters

Abstract

MERIS is designed for studies of coastal water quality. The retrieval of chlorophyll (CHL) in these waters (using other sensors) has presented problems due to a number of reasons, such as the difficulties in atmospheric correction over turbid waters. The bad discrimination of CHL at higher concentrations of CDOM and/or TSM also poses challenges to algorithm design. This paper reports on a sensitivity analysis of various analytical algorithms that all use spectral information of MERIS to retrieve CHL, TSM, and CDOM. Investigated are Matrix Inversion Methods (MIM), Ratio Matrix Inversion (RMI), Levenberg Marquardt methods (LM), and two new methods, namely Ratio Levenberg Marquardt and Hybrid Iterative Methods. All methods are direct inversions of the Gordon model. The test dataset comprised of 4 datasets of mean inherent specific optical properties collected in Dutch and Belgian Coastal waters. This data was used to parameterise the Gordon model, which was then used to generate spectra based also on random concentrations. To the simulated spectra errors were added of the following types: scaling errors, white errors, blue errors and errors in the Specific Inherent Optical properties (SIOP). A number of algorithms require a robust initial estimation of concentrations. Simple algorithms for this purpose are presented. The results show that Hybrid Iterative Methods in general perform well. A wrong choice of SIOP-set causes the largest errors in concentration retrieval in all methods.

2.1 Basics of forward and inverse modelling: The Gordon model and the SIOP model

Bio-optical models describe the relationship between the amount of upwelling light just below the water surface (here expressed as subsurface irradiance reflectance) and the optical properties of water and its optical active constituents. For this study it is assumed that the optical active constituents groups are: 1) TSM: Total Suspended Matter; 2) TCHL: Total Chlorophyll and 3) CDOM: Chromophoric Dissolved Organic Matter. In most cases this is a workable assumption, especially because the optical properties of these groups can be determined relatively easy and unambiguously. If red tides or e.g. cyanobacterial blooms are present, this assumption no longer holds. Overviews of optical models to describe light propagation in water can be found in Gordon (1975). Analytical model inversion schemes benefit from simplified models. Therefore, in a number of studies of turbid inland and coastal waters, use has been made of a version of the Gordon (1975) reflectance model to predict the subsurface irradiance reflectance $R(0^-)$:

$$R(0^-) = f \cdot \frac{b_b}{a + b_b}$$

(**Fout! Opmaakprofiel niet gedefini**

eerd..1)

f may vary due to solar and viewing geometry; for this study it is set at 0.38 (see e.g. Dekker et. al., 2001). For the inversion of actual spectra *f* should be estimated. Additional assumptions are that the medium is optically deep and completely mixed. Inelastic scattering effects such as Raman scattering and fluorescence are ignored. Peters et al. (2001) showed that (for a number of North Sea spectra) good matches between observed and modelled spectra can be achieved with the Gordon model if the main scaling parameters (model: *f* and *B;* observed spectra: *Q* and r_{sky}) are correctly parameterised. It is assumed that the inherent optical properties (IOPs): *a* and b_b (respectively absorption and backscattering) are linear functions of the constituents' concentration which allows defining Specific Inherent Optical Properties (SIOP) as: SIOP = IOP/C_{is} (C_{is} is the in situ measured concentration of the respective constituent). This normalization of in situ measured IOPs allows to estimate the IOP at any (model) concentration (C_m) from: IOP = C_m * SIOP. So *a* and b_b of natural water are expressed in terms of the constituents of the water as follows:

$$a = a_w + a^*_{TCHL} \cdot TCHL + a^*_{TSM} \cdot TSM + a^*_{CDOM} \cdot CDOM$$

(**Fout! Opmaakprofiel niet gedefinieerd.**.2)

$$b_b = b_{b,w} + Bb^*_{TSM} \cdot TSM$$

(**Fout! Opmaakprofiel niet gedefinieerd.**.3)

The set of equations 1, 2 and 3 provides an explicit relationship between the SIOP, the concentrations of the water constituents and $R(0^-)$. All backscattering is lumped as total particulate backscattering. Since phytoplankton backscattering is decoupled from phytoplankton absorption unrealistic simulations may occur at high TCHL concentrations and (very) low TSM values, e.g. algal bloom situation. This situation does not occur in the concentration ranges that are part of this simulation study.

2.2 Set-up of the sensitivity analysis

In the sensitivity analysis the influence of a number of error-types on the concentration retrieval was tested. In general 1000 sets of random concentrations were generated in the following concentration ranges: TSM: 1-50 g m^{-3}, TCHL: 1-40 mg m^{-3}, CDOM 0.1 – 1.5 m^{-1}. Using a random choice from a set of 4 cruise-mean SIOP-sets (see figures 1a, 1b, 1c and 1d) 1000 input spectra were simulated. In 5 steps the spectra were increasingly deteriorated using one of the following errors:

1. Scaling error: implemented as $f_{inverse}$ = (0.34 ; 0.36 ; 0.38; 0.40; 0.42)

2. White error: implemented as $R(0-,\lambda) = R(0-,\lambda) + (0; 0.00125; 0.0025; 0.00375; 0.005)$
3. Blue error: implemented as $R(0-,\lambda) = R(0-,\lambda) – X.\lambda^{-1.5}$ (X = 0..4)
4. SIOP error: in order to test the general sensitivity to SIOP errors the spectra were inverted using a mean SIOP-set based on the three input-sets.

The influence of these 4 error-types on concentration retrieval was tested separately and in a 'worst case' analysis all lumped together. For a first review of these algorithms, the result of the analysis is presented by the correlation coefficient (r^2).

2.3 Types of Analytical algorithms tested

1) Existing analytical inversion schemes: This study features the sensitivity analysis of 4 types of existing analytical inversions of water spectra, namely:

1. 1-band – one parameter inversion (for TSM retrieval using the MERIS band at
2. 704 nm: ***TSM-1b-704***, Van der Woerd et al., 1999)
3. Matrix Inversion (***MIM***: Hoge and Lyon, 1996)
4. Levenberg Marquardt (***LM***)
5. Ratio Matrix Inversion (***RMI***: Peters et al., 2001). Note that ***RMI*** is non-linear in TSM, which means that in addition to the matrix inversion itself a predictor-corrector method is used to estimate TSM.

Note that ***MIM***, ***LM*** and ***RMI*** can be used as 3, 2 or 1-parameter algorithms with required initial estimations of the non-retrieved parameters.

2) RLM: A new inversion scheme: For this study one new inversion type was attempted, namely Ratio Levenberg Marquardt (***RLM***). ***RMI*** and ***RLM*** use as input a spectrum of band-ratios derived from the input spectrum (each possible ratio exists precisely once in the ratio spectrum).

3) HIM: Already mentioned by Peters et al. (2001), a new category of analytical inversion methods is Hybrid Iterative Inversion Methods (***HIM***). Some examples of this type of algorithm have been implemented experimentally in this study.

2.4 Hybrid Iterative Inversion Methods (*HIM*)

The general principle of ***HIM*** is that (for TSM, TCHL and CDOM) separate, 1-parameter multi band analytical inversion methods are used in an iterative scheme. A rationale for this approach is the fact that TCHL and CDOM can probably best be retrieved by methods based on band ratios, while TSM is probably best retrieved by linear methods. There are two conditions to ***HIM***, namely: 1) for the first step one needs initial values of two parameters and 2) the iterative process must converge. Based on the above-described analytical inversion methods the 5 ***HIM***-experiments were implemented (see Table 2.1).

2.5 Initial estimations of TCHL, TSM and CDOM

Some analytical algorithms like LM require or benefit from a robust and reasonably exact initial estimation. A number of algorithms presented in this paper have TCHL, TSM or CDOM as a free parameter and require estimations of one or two of the other parameters. HIM requires initial estimates of two parameters.

2.5.1 Initial CHL

There is a long history of CHL-estimation using band ratios. Input bands for case-2 waters are usually centered on the CHL-absorption maximum around 667 nm and around 705 nm (reference band). A useful algorithm was published by Gons (1999) based on the following assumptions: 1) At 700 nm and further in the infrared the only two factors that influence R(0-) are a_w and b_b; therefore observations beyond 700 nm can be used to estimate b_b directly from R(0-). 2) At 676 nm R(0-) is influenced by a_w, a_{TCHL} and b_b. For this study we redefine the Gons algorithm for CHL-a to (dropping the empirical constant p; normalizing pigment absorption using TCHL instead of CHL-*a*; using the 665 nm band instead of 672 nm and the 704 band instead of e.g. the 754 nm band):

$$TCHL = \left(\frac{R(0^-)_{704}}{R(0^-)_{665}} \left(a_{w,704} + b_b \right) - a_{w665} - b_b \right) / \left(a^*_{TCHL,665} \right) \quad \text{(Fout! Opmaa kprofiel niet gedefini eerd..4)}$$

For application with MERIS we take the 704 nm band to determine b_b according to:

$$b_b = \left(\frac{R(0^-)_{704}}{f} a_{w,704} \right) / \left(1 - \frac{R(0^-)_{704}}{f} \right) \quad \text{(Fout! Opmaa kprofiel niet gedefini eerd..5)}$$

Note that for this simulation study it is sufficient to fix *f*; for application with satellite data *f* needs to be calculated as function of the solar and viewing geometry. The TCHL-specific pigments absorption at 665 nm was determined as the mean value from the three described cruises in Dutch-Belgian national waters: $a^*_{TCHL,665}$=0.0115 which is significantly lower than the inland waters value derived by Gons (0.0176). Note that ratio algorithms are relatively insensitive to errors in b_b, which means that with $a_{w,704}$ = 0.658 and f=0.38, b_b can be approximated as:

$$b_b = 2.3 R(0^-)_{704} \quad \text{(Fout! Opmaa kprofiel niet gedefini eerd..6)}$$

2.5.2 Initial CDOM

It is difficult to define robust but efficient CDOM algorithms because the CDOM influence on the spectrum is masked by the influence of other constituents in almost all regions of the spectrum. Here we developed an algorithm based on the following assumptions: 1) CDOM can best be calculated from a band ratio; 2) the exact band choice is less important; 3) b_b is spectrally neutral and equation (6) can be used to estimate b_b and 4) the sum of a_w; a_{TCHL} and a_{TSM} is treated as an empirical constant. A ratio of two spectral bands based on equations 1, 2 and 6 leads to:

$$CDOM = \left(c_{443} - R \cdot c_{561} + 2.3 \cdot R(0^-)_{704} - R \cdot 2.3 \cdot R(0^-)_{704}\right) / \left(R \cdot a^*_{CDOM,561} - a^*_{CDOM,443}\right) \quad (\textbf{Fout! Opmaakprofiel niet gedefinieerd.}.7)$$

With $R = \dfrac{R(0^-)_{561}}{R(0^-)_{443}}$ and

$$c_\lambda = a_{w,\lambda} + TCHL \cdot a^*_{TCHL,\lambda} + TSM \cdot a^*_{TSM,\lambda} \quad (\textbf{Fout! Opmaakprofiel niet gedefinieerd.}.8)$$

Where λ is 561 and 443. From SIOP analysis it was found that $c_{443} \cong 2 \cdot c_{561}$ and from regression analysis (based on spectra simulated using random concentrations and 4 random SIOP sets) it was found that $c_{561} \cong 0.1196$.

2.5.3 Initial TSM

For initial North Sea TSM estimations a one-band inversion of the Gordon model is very suitable (Van der Woerd et al., 1999). The MERIS band around 704 nm is the most suitable for TSM estimations since the relationship R(0-) vs. TSM at this wavelength is linear and does not saturate at higher concentrations. For the parameterization either global/regional mean or location-specific SIOPs can be used. The TSM algorithm needs initial estimates of CHL and CDOM, although the sensitivity to errors in both parameters is low.

2.6 In-situ measurements

In three campaigns 39 samples were analysed for concentrations of TCHL, TSM and CDOM (Figure 2.1), above water measured spectra of subsurface irradiance reflectance ($R0^-$) and IOPs (Peters et al., 2001)(table 2.2) The set of measurements in Belgian coastal waters was split in a high TSM and a low TSM set. Of the four resulting sets cruise-mean SIOPs were calculated and used for the sensitivity study (Figure 2.2).

2.6.1 (S)IOP measurement methods

TCHL (chlorophyll-a plus phaeopigment) was determined spectrophotometrically after pigments extraction using hot ethanol (80%, 75^{o}C). TSM was determined by filtering samples over Whatman GF/F filters and drying the filters at 80^{o}C. Ignition loss was determined by ashing the filters with TSM at 550˚C. The filters were flushed with tap water to remove salt. The absorption of CDOM was determined (after filtration through a Whatman GF/F filter) from optical density measurements in a 5-cm cuvette. CDOM concentrations are expressed as the absorption at 440 nm. Total absorption (*a*) and beam attenuation (*c*) were measured in a 5 cm cuvette using a double-beam spectrophotometer. All spectra were measured between 350 and 750 nm, at 1-nm intervals. Absorption spectra of TSM and bleached TSM were determined using the filter pad method with Whatman GF/F filters. The filter was bleached using hot ethanol (80 %, 75^{o}C). The extinction at 750 nm was subtracted from the entire spectrum, as a correction for residual scattering. Subtracting the bleached TSM absorption from the TSM absorption gave the TCHL absorption spectrum. Subtraction of total absorption (TSM + CDOM absorption) from beam attenuation gave the total scattering. All measurements were performed by M. Rijkeboer and are described in Peters et al. (2001).

2.7 MERIS band settings

Selected MERIS bands for this study were the spectral bands at 412.5, 442.5, 490, 510, 560, 665 and 705 nm. The 681.25 and 620 nm band were omitted because fluorescence and cyanophycocyanin absorption are not incorporated in the forward and inverse model. The 754 nm band was omitted because the water leaving radiance in this band will be very low. Analysis using this spectral band is hampered by the fact that a number of SIOPs (a_{TSM}, a_{TCHL}, and a_{CDOM}) are measured only to 750 nm.

2.8 results and discussion

Table 2.4 shows the resulting r^2 of all tested algorithms (MIM, RMI, LM, RLM and HIM1-5). InitTSM is the result of the 1-band-704 algorithm fed with the initCHL and initCDOM estimations. Next InitCDOM estimations were improved by feeding initTSM and initCHL into the RLM1CDOM algorithm. InitTSM estimations are not improved by iteration in HIM-schemes, which will have influenced the outcome for TSM and CDOM because the iteration criterion was based on changes in TSM. InitCDOM estimations are only improved by other algorithms in case of SIOP errors. RMI appeared to be unstable at TSM<5, hence the lower r^2 values in a number of tests. Ratio based methods give, as

expected, good results for CHL and CDOM. The LM method also gave excellent TCHL retrieval, especially in the HIM-4 scheme. All analytical methods are relatively sensitive to errors in SIOP-choice. The adapted Gons-TCHL algorithm (initCHL) was parameterized with a mean $a^*_{TCHL,665}$ which explains the lower starting value (r^2 0.84). In the worst-case analysis this algorithm performs best. The best HIM variants are HIM-4 and HIM-1. Some conclusions from this analysis are:

1. The initialisation algorithms perform very good and result in overall high correlations in the analytical algorithms.
2. Initial CDOM gave the worst initial estimation and was improved by an additional step consisting of the RLM1CDOM algorithm. It was however sufficient to initialise the 1band-704 TSM algorithm.
3. Classic MIM methods are less suitable for TCHL estimations in cases of white and SIOP errors. RMI results are affected by instabilities in low-TSM concentration retrieval. RLM. LM-TSM estimations are equal in quality to initTSM estimations.
4. The closer the SIOP that is used for inversion is to the actual SIOP set, the better. Methods should be investigated to estimate SIOPs from the images themselves.
5. Ratio LM is very useful for CDOM estimations. TSM estimations in HIM-schemes are unstable with almost all algorithms except the 1band-704 algorithm.
6. Although further testing is required, the optimum algorithm for all conditions seems to be a combination of TSM: initTSM; TCHL: initCHL or LM1CHL and CDOM: MIM1cdom in a non-iterative scheme.

Improvements in the tests could be: HIM-iteration criterion based on TCHL-changes, Blue error better specified, more SIOP-datasets, use of SIOP-models to test the sensitivity to errors in individual SIOPs.

*Table **Fout! Opmaakprofiel niet gedefinieerd.**.1 Sequence of 1-parameter algorithms in a number of Hybrid Iterative Inversion Methods experiments.*

	Step 1	Step 2	Step 3
HIM1	TSM-1b-704	RMI1CDOM	RMI1CHL
HIM2	TSM-1b-704	LM1CHL	RMI1CDOM
HIM3	TSM-1b-704	LM1CHL	LM1CDOM
HIM4	TSM-1b-704	LM1CHL	RLM1CDOM
HIM5	LM1TSM	LM1CHL	RLM1CDOM

*Table **Fout! Opmaakprofiel niet gedefinieerd.**.2 Logistical information of in-situ sampling campaigns.*

Vessel	Date	#Samples	Location description
Mitra	May 8+9, 2000	8	Noordwijk Transect, The Netherlands. Lat: 52° 05' - 52° 18' N; Lon: 4 °15' - 4 °18' E
Navicula	May 22+23, 2000	12	Marsdiep, The Netherlands Fixed location Lat: 52.58 N; Lon: 4.46 E
Belgica	April 17, 18+19, 2000	19	Belgian coastal waters Lat: 51° 09' - 51° 30' N; Lon: 2 °36' - 3 °19' E

*Table **Fout! Opmaakprofiel niet gedefinieerd.**.3 Mean concentrations for 4 cruise mean SIOP-datasets and mean estimated B.*

	Belgica-2000-I	Belgica-2000-II	Mitra-2000	Navicula-2000
TCHL	12.7	18.7	25.0	23.2
TSM	17.1	51.9	8.0	10.3
CDOM	0.27	0.39	0.31	0.80
B	0.016	0.016	0.025	0.020

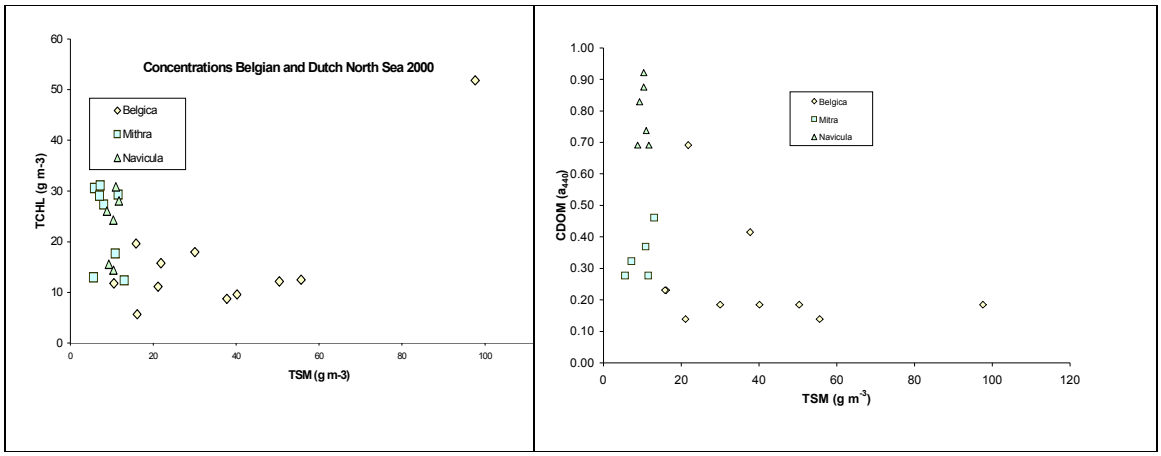

Figure 2.1 Scatter plots of TSM versus TCHL concentrations (Fig 2.1.a) and TSM versus CDOM concentrations (Fig 2.1.b).

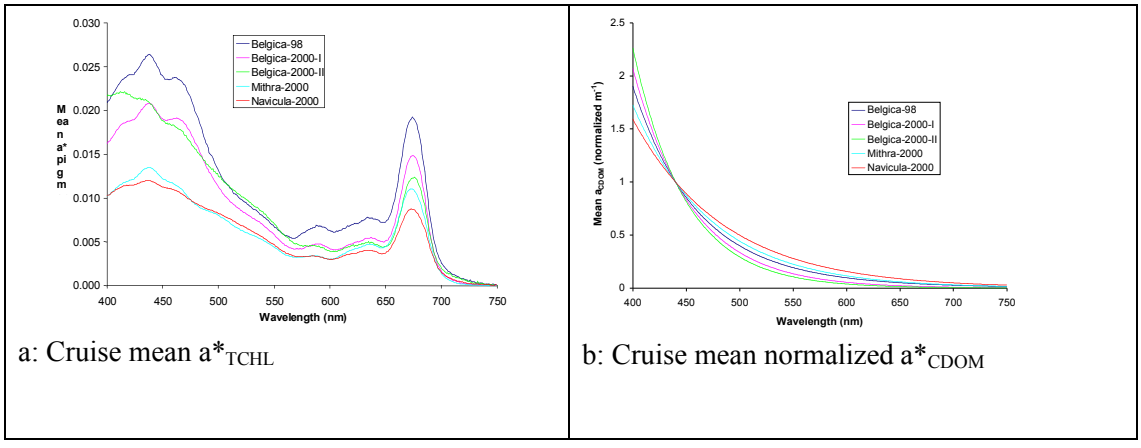

a: Cruise mean a^*_{TCHL}

b: Cruise mean normalized a^*_{CDOM}

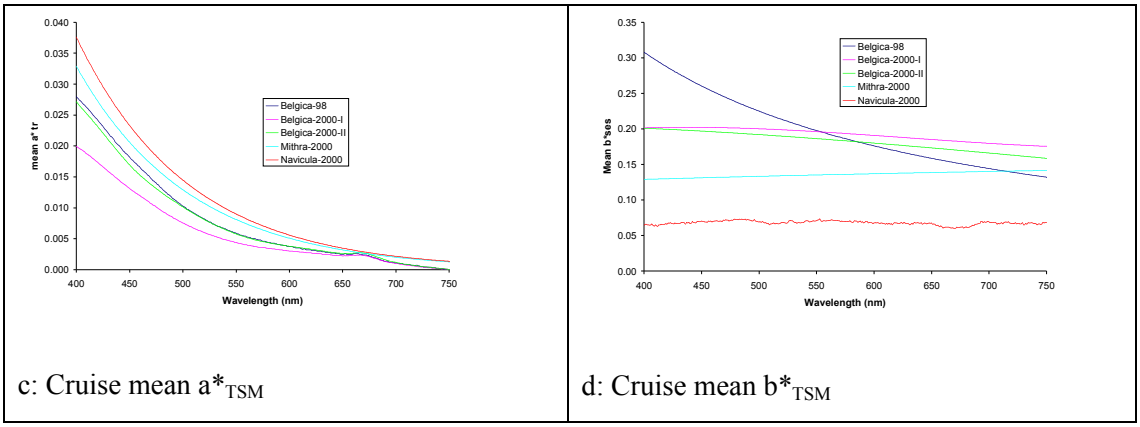

c: Cruise mean a^*_{TSM}

d: Cruise mean b^*_{TSM}

Figure 2.2 Average cruise spectra for a^*_{TCHL}, a^*_{CDOM}, a^*_{TSM}, b^*_{TSM}.

*Table **Fout! Opmaakprofiel niet gedefinieerd.**.4 Results for r^2 of the sensitivity analysis for TCHL, TSM and CDOM.*

	No-error			Scaling error			White error			Blue error			SIOP-error			All-errors		
	TCHL	TSM	CDOM	TCHL	TSM	CDOM	TCHL	TSM	CDOM	TCHL	TSM	CDOM	TCHL	TSM	CDOM	TCHL	TSM	CDOM
MIM3	1.00	1.00	1.00	1.00	1.00	1.00	0.92	1.00	0.86	0.98	1.00	0.99	0.70	0.82	0.94	0.73	0.80	0.77
MIM2	0.93	1.00		0.90	1.00		0.62	0.99		0.93	1.00		0.62	0.81		0.26	0.77	
MIM1CHL	0.86			0.85			0.65			0.86			0.44			0.38		
MIM1TSM		1.00			1.00			0.99			1.00			0.84			0.84	
MIM1CDOM			0.98			0.97			0.89			0.97			0.93			0.88
RMI3	1.00	0.99	0.95	1.00	0.99	0.95	0.96	0.72	0.52	0.97	0.78	0.67	0.84	0.46	0.43	0.76	0.34	0.25
RMI2	1.00		1.00	1.00		1.00	0.86		0.86	0.99		0.99	0.93		0.93	0.76		0.76
RMI1CHL	0.97			0.96			0.64			0.95			0.67			0.26		
RMI1TSM		0.92			0.89			0.87			0.91			0.35			0.33	
RMI1CDOM			1.00			1.00			0.87			0.99			0.93			0.79
LM3	1.00	1.00	1.00	1.00	1.00	1.00	0.88	1.00	0.92	1.00	1.00	1.00	0.78	0.84	0.72	0.59	0.84	0.64
LM2	0.97	1.00		0.97	1.00		0.96	1.00		0.97	1.00		0.82	0.84		0.78	0.84	
LM1CHL	0.97			0.97			0.98			0.97			0.87			0.83		
LM1TSM		0.99			0.99			0.99			0.99			0.83			0.83	
LM1CDOM			0.89			0.88			0.81			0.89			0.63			0.65
RLM3	1.00	1.00	1.00	1.00	1.00	1.00	0.39	0.79	0.24	1.00	1.00	0.99	0.90	0.63	0.69	0.35	0.41	0.16
RLM2	1.00		1.00	1.00		1.00	0.93		0.96	1.00		1.00	0.83		0.68	0.74		0.72
RLM1CHL	0.98			0.98			0.97			0.98			0.83			0.78		
RLM1TSM		1.00			1.00			0.99			1.00			0.91			0.86	
RLM1CDOM			0.97			0.96			0.90			0.97			0.65			0.69
InitTSM		1.00			1.00			1.00			1.00			0.84			0.84	
InitCDOM			0.97			0.96			0.90			0.97			0.65			0.69
InitCHL	0.84			0.86			0.86			0.85			0.86			0.85		
HIM-1	1.00	1.00	1.00	1.00	1.00	1.00	0.93	1.00	0.86	0.98	1.00	0.99	0.74	0.84	0.93	0.80	0.84	0.76
HIM-2	1.00	1.00	1.00	1.00	1.00	1.00	0.80	1.00	0.81	0.99	1.00	0.99	0.50	0.85	0.93	0.43	0.84	0.62
HIM-3	1.00	1.00	1.00	1.00	1.00	1.00	0.86	1.00	0.92	1.00	1.00	1.00	0.75	0.84	0.72	0.56	0.84	0.64
HIM-4	1.00	1.00	1.00	1.00	1.00	1.00	0.95	1.00	0.96	1.00	1.00	1.00	0.81	0.84	0.70	0.73	0.84	0.74
HIM-5	0.98	1.00	0.99	0.89	1.00	0.98	0.91	1.00	0.90	0.37	0.58	0.59	0.55	0.83	0.66	0.60	0.68	0.56

3. Results from MERIS rehearsal

Before the launch of MERIS the MERIMON team participated in a number of workshops to update measurement protocols, to calibrate and compare instruments and to do a rehearsal of the upload of validation measurements to the MAVT-NILU database. The measurement protocols are an update of the SeaWiFS protocols (Fargion, 2000; McClain, 2000; Mueller, 2000) described in the regular ESA publications (Doerffer, 2002). It is important to note that these protocols were elaborated upon in the EC FP5 REVAMP project (Tilstone et al., 2003; in preparation). In this chapter we report on the inter-calibration activities of above-water reflectance measurements at the PlymCal workshop in 2001. These measurements are employed in the MERIS validation (see Chapter 4). An overview of the participants of the workshop is shown in Figure 3.1. The following paragraphs describe MERIMON specific activities employed during the workshop. General workshop findings are discussed in the last paragraph of this chapter.

*Figure **Fout! Opmaakprofiel niet gedefinieerd.**.1 Participants of the PlymCal 2001 workshop.*

3.1 Radiometric calibration of the PR-650

The IVM PR-650 (Photo research Spectrascan PR650 S/N: 60012202) was calibrated in the optics lab (dark room) of PML at 16/08/2001 17:30 (UTC+1). The calibration set-up comprised a calibrated lamp and a calibrated Lambertian reflectance plaque, as indicated in the following figure. The most recent calibration prior to the MAVT intercalibration workshop was the factory calibration, performed 21/06/2001.

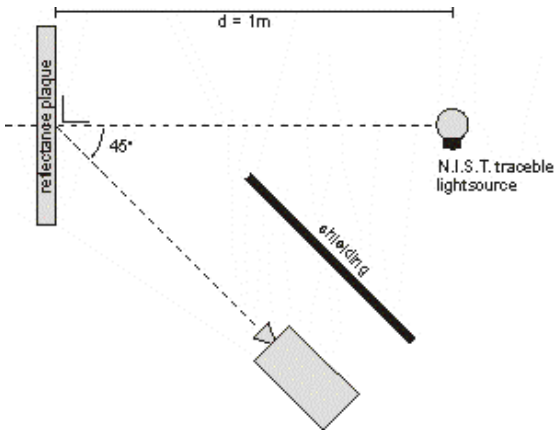

*Figure **Fout! Opmaakprofiel niet gedefinieerd.**.2 Set-up used for the absolute radiometric calibration of the IVM PR-650.*

The results are shown in the following figure, showing two lines, one (blue) being the radiance measurement based on the existing calibration dated 21/06/2001, corrected for straylight, and one (red) being the theoretically derived radiance based on the lamp output, spectral reflectance of the plaque for 45° observing angle and the distance from the lamp to the plaque. The figure on the right shows the ratio between the two calibrations.

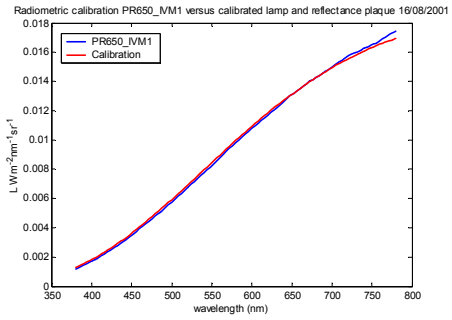

a)

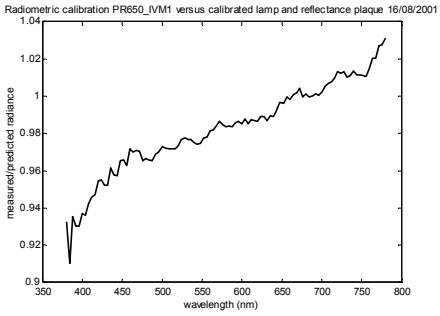

b)

Figure 3.3 Results for the radiometric calibration of the PR-650. a) Measured radiance based on current calibration (blue) and theoretically derived radiance. b) Ratio of the two calibrations.

Because of the large dynamic range of the PR-650, a linearity calibration would be advisable in future (note that the differences between the radiances measured between one measurement cycle (water, sky, reflectance panel) for a particular wavelength can be a factor 200).

3.2 Field campaign results

At 15 and 16 August 2001 IVM and MUMM participated in the field cruise on the MS Squila, organised by the Plymouth Marine Laboratories. A total of 19 measurement series were obtained near the coast of Plymouth (see Figure 3.4), covering a range in water types, solar zenith angles and atmospheric conditions (Table 3.1).

Table 3.1 Coordinates and codes of sampling locations where reflectance spectra were taken by IVM.

Serial number	date	time	latitude	longitude
text	dd/mm/yy	hh:mm [UTC]	Minutes North of 50N	Minutes West of 4W
IVM1	15/08/01	09:09	20.65	9.16
IVM2	15/08/01	10:09	15.26	12.57
IVM3	15/08/01	10:30	15.52	12.67
IVM4	15/08/01	10:45	15.79	12.75
IVM5	15/08/01	11:45	15.08	12.65
IVM6	15/08/01	12:00	15.03	12.76
IVM7	15/08/01	12:15	15.1	12.74
IVM8	15/08/01	13:00	20.1	9.12
IVM9	15/08/01	13:30	21.42	10.23
IVM10	16/08/01	08:50	21.74	10.12
IVM11	16/08/01	08:55	21.71	10.18
IVM12	16/08/01	09:10	21.82	10.34
IVM13	16/08/01	09:25	21.73	10.24
IVM14	16/08/01	09:50	21.68	10.25
IVM15	16/08/01	10:10	21.79	10.20
IVM16	16/08/01	10:45	20.27	9.40
IVM17	16/08/01	11:00	20.23	9.36
IVM19	16/08/01	13:20	15.38	11.34

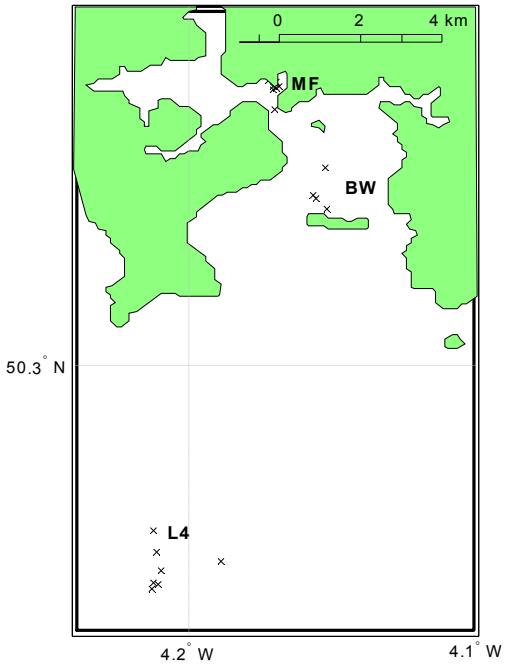

*Figure **Fout! Opmaakprofiel niet gedefinieerd.**.4 Approximate codes used by PML (bold) and IVM sampling locations (x).*

Based on the summary of the above water datasets acquired by MUMM during the Squilla cruise, the following concurrent locations were selected.

*Table **Fout! Opmaakprofiel niet gedefinieerd.**.2 Selected measures.*

Date		MUMM			IVM	
d/m/y	Station	Starttime	Finishtime	Cast	Station	Time
15/8/2001	L4_15_A	10:22	10:29	#2/4	IVM3	10:30
16/8/2001	MA_16	9:15	9:23	#2/4	IVM13	9:25
16/8/2001	L4_16	13:15	13:26	#1/1	IVM19	13:20

To get a feeling about how stable weather conditions were during these measurements, digital photos were made of both the sky and water during the PR-650 measurements.

The sky was completely diffuse (at least approximately in the direction of the sensor) for stations IVM3 (completely clouded) and IVM19 (cloud-free). For MERIS validation the clouded sky is irrelevant, moreover, the sky reflectance measurement is expected to be less accurate due to the (relatively) larger contribution of sky reflected radiance to the total upwelling radiance in air above water.

3.3 Comparison IVM3 vs. L4_15_A

There was a small time difference between the measurements of MUMM and the measurement of IVM. It is also important to note that the sensor is aimed manually for the IVM method, whereas for the MUMM method the sensor is rigidly attached to the vessel's bow, so aiming depended on the ship's orientation with respect to the sun.

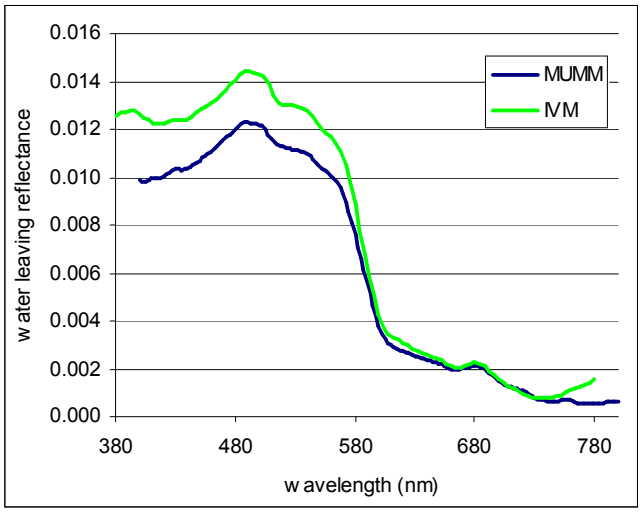

*Figure **Fout! Opmaakprofiel niet gedefinieerd.**.5 Comparison between water leaving reflectance measurements by MUMM and by IVM at station L4, August 15, 2001 around 10:30 UTC.*

The spectra match excellent in the red but have a difference of approximately 0.002 in the blue part of the spectrum.

The difference might be due to natural variability in the water-leaving reflectance (vertical, horizontal or temporal variations can be considered because measurements were not exactly synchronized but were captured during several minutes), or due to direct measurement errors (aiming of the sensor, straylight, radiometric issues). In this respect it is also interesting to take a look at the standard deviation following from the three repeated measurement cycles of the PR-650 method. Two methods can be considered to obtain a standard deviation in the water leaving reflectance:

1. Calculation of the reflectance per measurement cycle and then taking the mean and standard deviation
2. Calculation of the mean and standard deviation of each radiometric measurement (L_w, L_{sky}, E_d) and then translate these statistics to the reflectance measurement according to

$$\langle \rho_w \rangle = \pi \frac{\langle L_u \rangle - r_{sky} \langle L_{sky} \rangle}{\langle E_d \rangle}$$

$$\left[\frac{\Delta\rho}{\pi}\right]^2 = \left[\frac{\Delta L_u}{\langle E_d \rangle}\right]^2 + \left[\frac{-r_{sky}\Delta L_{sky}}{\langle E_d \rangle}\right]^2 + \left[\frac{-\Delta E_d}{\langle E_d \rangle}\rho_w\right]^2$$

(**Fout! Opmaakprofiel niet gedefinieerd.**.1)

Where the Δ indicated the standard deviation, and the brackets $\langle L \rangle$ indicated the mean value.

Results are indicated in the following figure, where the superscripts 1 and 2 denote the method used for the calculation of the PR-650 statistics and σ denotes the standard deviation. The grey bands show the area plus and minus one standard deviation. The MUMM concurrent measurement is shown for comparison.

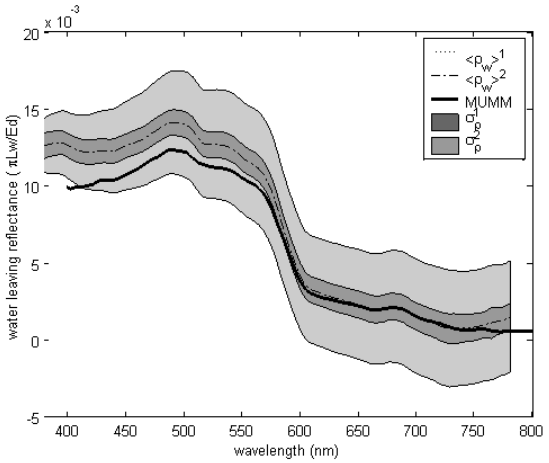

*Figure **Fout! Opmaakprofiel niet gedefinieerd.**.6 Comparison between water leaving reflectance measurements by MUMM and by IVM with an indication of the typical errors.*

3.4 Comparison MA_16 vs. IVM13

Again a time difference of up to several minutes is possible.

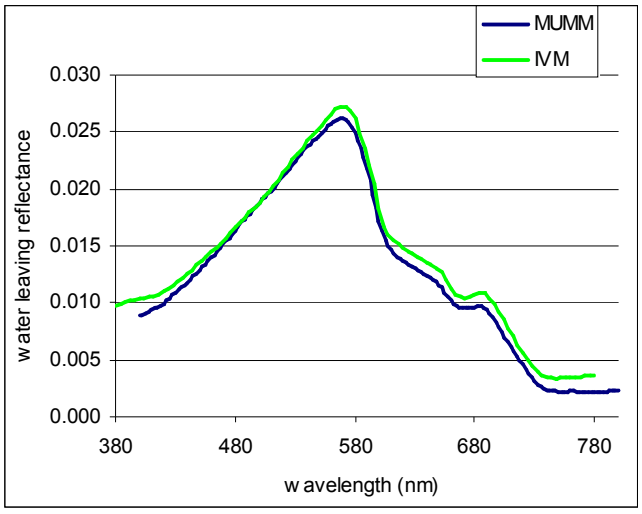

Figure ***Fout! Opmaakprofiel niet gedefinieerd.****.7 Comparison between water leaving reflectance measurements by MUMM and by IVM at station MA, August 16, 2001 around 9:25 UTC.*

The difference between the two spectra is smaller than 0.0016.

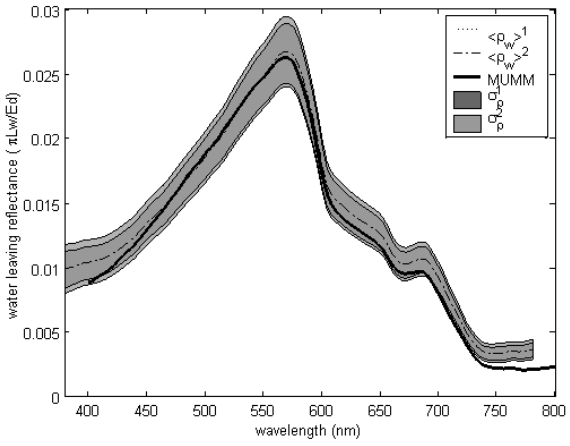

Figure 3.8 Comparison between water leaving reflectance measurements by MUMM and by IVM with an indication of the typical errors.

3.5 Comparison L4_16 vs. IVM19

The IVM measurement cycle was taken parallel with the MUMM measurement cycle.

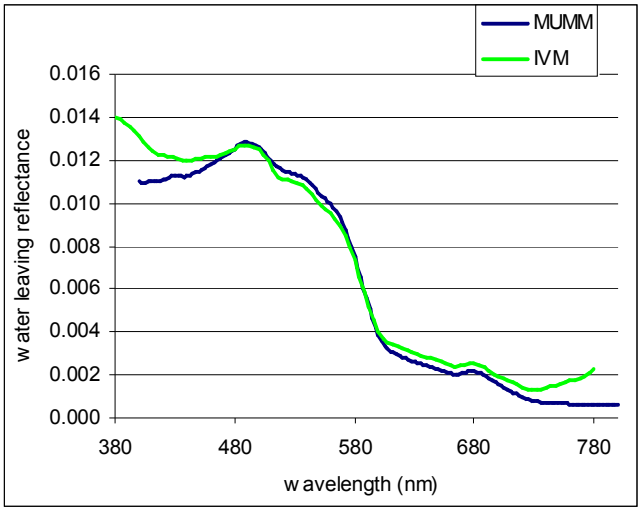

Figure 3.9 Comparison between water leaving reflectance measurements by MUMM and by IVM at station L4, August 16, 2001 around 13:20 UTC.

In the central part of the spectrum, the measurements compare excellent: the absolute difference is smaller than 0.001 between 425 and 755 nm. In the red and blue and of the spectrum the difference is significantly larger, but still smaller than 0.002.

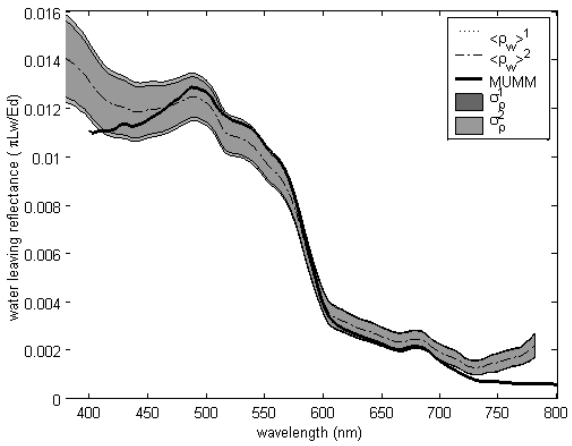

Figure 3.10 Comparison between water leaving reflectance measurements by MUMM and by IVM with an indication of the typical errors.

The unexpected increase in reflectance for $\lambda < 425$ and $\lambda > 755$ indicates an artefact in the PR650 method. The artefact was traced back to the opening or closing of the eyepiece (viewer) of the PR-650. Especially when aiming at the water without looking

through the eyepiece, stray light from above (skylight) can enter the PR-650 and reach the photo detector array. Note that this condition only is of importance in bright field conditions when making measurements of the water without looking through the eyepiece. For subsequent field campaigns the protocols were updated to use the eyepiece shutter when the operator does not look through the eyepiece.

3.6 Summary and recommendations

The PlymCal I workshop has resulted (in combination with other activities) in three major developments within the MERIS and AATSR Validation Team and the REVAMP project:

1. Acceptance of above water reflectance measurements in support of MERIS geophysical level 2 products validation.
2. Further optimisation and definition of measurement protocols for REVAMP (Tilstone et al., 2002), and to a lesser extend the MAVT.

4. MERIS validation of geophysical ocean colour products: preliminary results for the Netherlands

Abstract

Three field cruises were performed in 2002 for the validation of the geophysical ocean colour products of the MERIS sensor on board ENVISAT. At each cruise four stations were visited, where one of the stations was optimised to coincide with a MERIS overpass. Cloud-free sky conditions were realized during two cruises in April and September. For the cruise of 2 September 2002 a level-2 MERIS image was received and the geophysical products were compared with the in situ measured parameters. Two stations were measured within 1 hour of the MERIS overpass (1 and 50 minutes difference). The reflectance and suspended sediment concentration retrieved from the MERIS image were reasonably consistent with in situ observations. The MERIS algal pigment 2 was significantly higher and the yellow substance absorption was significantly lower than the in situ observations.

Only two match-up pixels are presented in this paper, so no statistically sound conclusive remarks can be made about the validation level of MERIS for the geophysical products that are discussed. Combination with other match-up pixels under different atmospheric conditions and for different concentration ranges are necessary to gain more insight in the MERIS accuracy. More in-depth research is needed to understand the nature of the differences between in situ and MERIS observations.

4.1 Introduction

In March 2002, the European Space Agency launched ENVISAT, a polar-orbiting Earth observation satellite that provides measurements of the atmosphere, ocean, land, and ice. The MEdium Resolution Imaging Specrometer Instrument (MERIS) on board ENVISAT is dedicated to measurements of sea colour in the oceans and in coastal areas. Knowledge of the sea colour can be converted into a measurement of chlorophyll pigment concentration, suspended sediment concentration and yellow substance absorption over the marine domain. There is a Dutch interest (RIKZ) in validated MERIS products for management of the coastal waters. Chlorophyll concentration and suspended matter concentration are regarded as key parameters in the study of phenomena such as eutrophication, harmful algal blooms, but also for the study of the effects of human interventions in the coastal area. Dutch national ship time was made available to the IVM team to participate in the validation of the MERIS water products in the framework of several research projects. The objectives of the field studies were:

1. To assess the accuracy of MERIS derived products (TCHL, TSM, CDOM) by making match-up measurements;
2. To report similarities and discrepancies to the European Space Agency;
3. To make recommendations to the European Space Agency about product improvements;

4. To inform the Dutch user community on the status and usefulness of MERIS products.

During the in-situ measurement campaigns data were acquired on water leaving reflectance, chlorophyll concentration, total suspended matter, yellow substance absorption and on inherent optical properties per station. In the analysis of MERIS imagery, also attention was given to some atmospheric parameters.

This paper describes the methodology and protocols used during the field sampling campaigns and the results of the comparison of MERIS observations with in-situ measurements.

4.2 Methodology

4.2.1 Cruise planning

The Institute for Environmental Studies was able to join the monitoring cruises in 2002 of the North Sea Directorate (a regional department of the Dutch Directorate-General of Transport, Public Works and Water Management) on a regular basis, provided it did not hamper the standard monitoring program. In practice, we were allowed to participate in one- or two-day cruises covering the so-called 'Noordwijk' transect, running from 2 to 70 kilometre offshore Noordwijk (52°15'N, 4°26'E). The decision to participate in a given cruise was determined by the prediction of the MERIS orbits and the weather conditions. This flexible approach was followed to maximise the chance of valid MERIS validation match-up stations with limited effort. The cruise overview is given in Table 4.1. Effectively 3 out of 15 cruises were joined, where the cruises of 8 April and 2 September had excellent weather and a MERIS overpass. The cruise of 3 June had cloudy weather and no MERIS overpass, but was carried out to improve the continuity over the summer of the measurements of concentrations and inherent optical properties. During each cruise four stations were visited, where one of those stations was synchronised with the predicted MERIS overpass.

4.2.2 Protocols

At each station a water sample was taken with a rosette sampler at 1 m depth, simultaneously with a surface reflectance measurement with a PhotoResearch PR650 spectroradiometer. Immediately after sampling the additional parameters were recorded, including wind speed and direction, time (UTC) and geographic position in UTM 31U projection, relative humidity, surface pressure, sky coverage, wave height, Secchi Disk depth, and any other observations that seemed relevant. Digital photos of sky and water coverage were also taken.

Reflectance is measured at least three times as quick as possible (typically within 3 minutes) to reduce effects of changing water masses and illumination conditions. Preferable position on the ship is on the bow, to minimize surface wave effects and shading and/or reflectance from the ship's superstructure. Each reflectance measurement consists of four radiance measurements (1) radiance emanating from the water surface L_t; (2) radiance from the sky L_{sky}; (3) radiance from the reflectance standard L_p; (4)

radiance from the shaded reflectance standard L_{pr}. A radiance measurement is an average of five readings, internally averaged by the radiometer. Measurement geometry is in accordance with findings by Mobley (1999) to minimize sky-reflectance as a function of wind speed. The view zenith and view azimuth (with respect to the sun) are $\theta_v = 40^o$ and $\phi_v = 135^o$, respectively. The sky radiance is measured (same geometry, but upward) to correct the total surface radiance for sky radiance reflected at the sea surface to yield water-leaving radiance $L_w = L_t - \rho_{sky} L_{sky}$, where ρ_{sky} is the effective Fresnel reflection coefficient for the wind-roughened sea surface. The radiance measurement of the reflectance standard is used to calculate above-water downwelling irradiance $E_{ad} = \pi \frac{L_p}{\rho_{panel}}$, where ρ_{panel} is the reflectance of the reflectance standard (~99%). The standard is measured under an angle of 45 degrees. The reflectance can than be calculated as $\rho_w = \frac{\pi L_w}{E_{ad}}$. The measurement of the shaded reflectance panel is not required for calculating MERIS reflectance, but can be used to get a handle on the downwelling radiance distribution (specifically the fraction diffuse/total downwelling irradiance F), which serves as input in numerical radiative transfer code such as Hydrolight.

Within half an hour after sampling the water was filtered for total suspended matter concentrations, chlorophyll concentrations and CDOM or yellow substance measurements. The chlorophyll filters were stored on board at less than -20°C, the raw water sample and filtrated water was stored in the dark at 4°C. After transportation to the laboratory the samples were analysed by AquaSense, for the following parameters within one day.

1. Total suspended matter concentration: filtration on a Whatmann GF/F pre-ashed (450°C) filters, rinsed with 3x50 ml MilliQ, and dried at 70° for 1 hour. Each sample was measured in triplicate;
2. Chlorophyll-a concentration[1]*: spectrophotometric method according to Dutch standard protocol (NEN 6520, 1981), each sample was measured in triplicate. For the MERIS validation the chlorophyll concentration was not corrected for phaeopigments;
3. Beam attenuation was measurement in a 10 cm cuvet using a single beam Ocean Optics spectrometer, referenced against milliQ;
4. Yellow substance absorption was measured after filtration over a Whatmann GF/F filter, in a 10 cm cuvet using an Ocean Optics spectrometer
5. (bleached) particle absorption was measured with the filterpad method (Trüper and Yentsch, 1967) on a Whatmann GF/F filter using an Ocean Optics spectrometer.

The phytoplankton pigment absorption was calculated as the difference of the particle absorption before and after bleaching. The particle scattering was calculated as the difference of the beam attenuation and the total absorption (particle absorption + yellow substance absorption). The protocols were updated in 2002 to comply as much as

[1] The AquaSense CHL-a measurements have been compared to other MAVT labs in the NIVAcal Round Robin experiment.

possible with REVAMP and MERIS validation protocols (Tilstone and Moore, 2002; Doerffer, 2002).

4.2.3 Used software & tools

All digital image processing was performed using Matlab 6.5 (R13). The MERIS measurement datasets were imported into Matlab using the MATBX (0.8.4) Java API (a prior version of BEAM 1.0). The appropriate row- and column indices for the match-up pixels were found by triangle-based, cubic interpolation in the latitude and longitude tie-point grids.

4.3 Available Imagery

In advance of the Envisat validation workshop in Frascati (9-13 December 2002) we received a MERIS image that was acquired on 2 September 2002 at 10:29:52 UTC. A true-colour quick look of the image of 2 September is given in Figure 4.1. The image was processed using the latest 'smile' correction and with the absorbing aerosol models switched off.

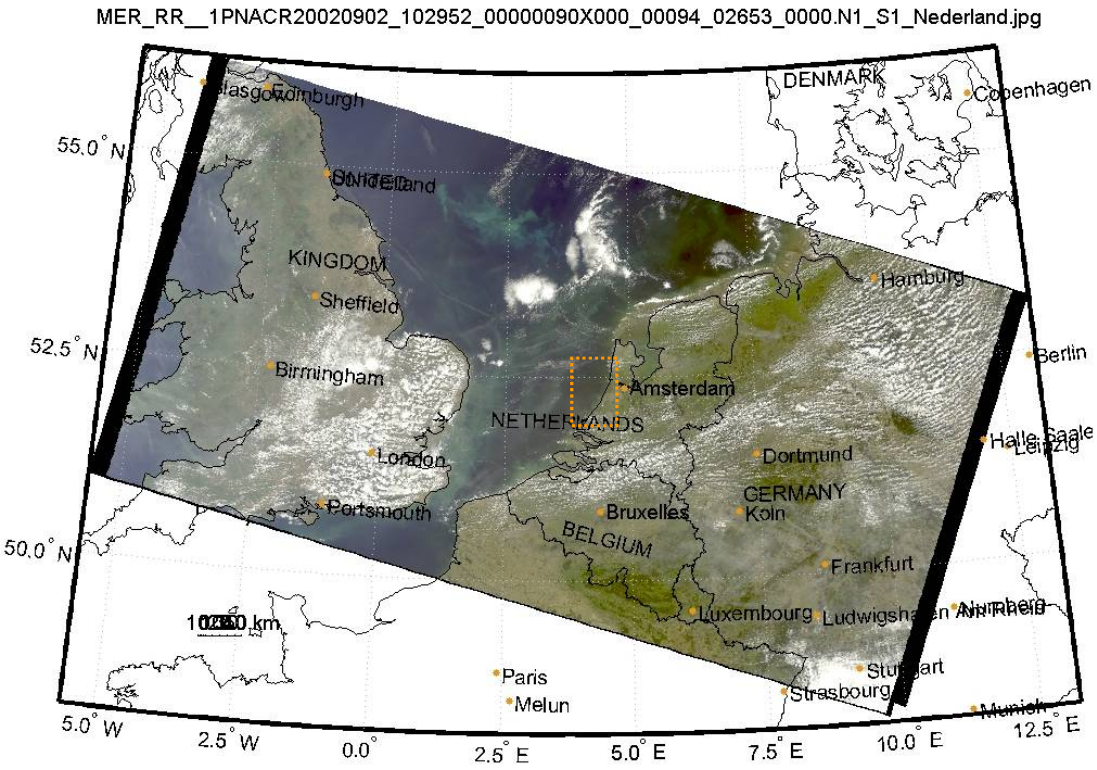

*Figure **Fout! Opmaakprofiel niet gedefinieerd.**.1 True-colour quick look of the MERIS image acquired 2 September 2002 at 10:29 above the North Sea. The subset of the image presented in Figure 4.5 is indicated by an orange dotted rectangle.*

The atmosphere was very clear at the time of MERIS overpass. A CIMEL station close (less than 15 km) to the match-up location indicated values of aerosol optical thickness of 0.1 (courtesy Marcel Moerman, TNO-FEL), as indicated in Figure 4.2.

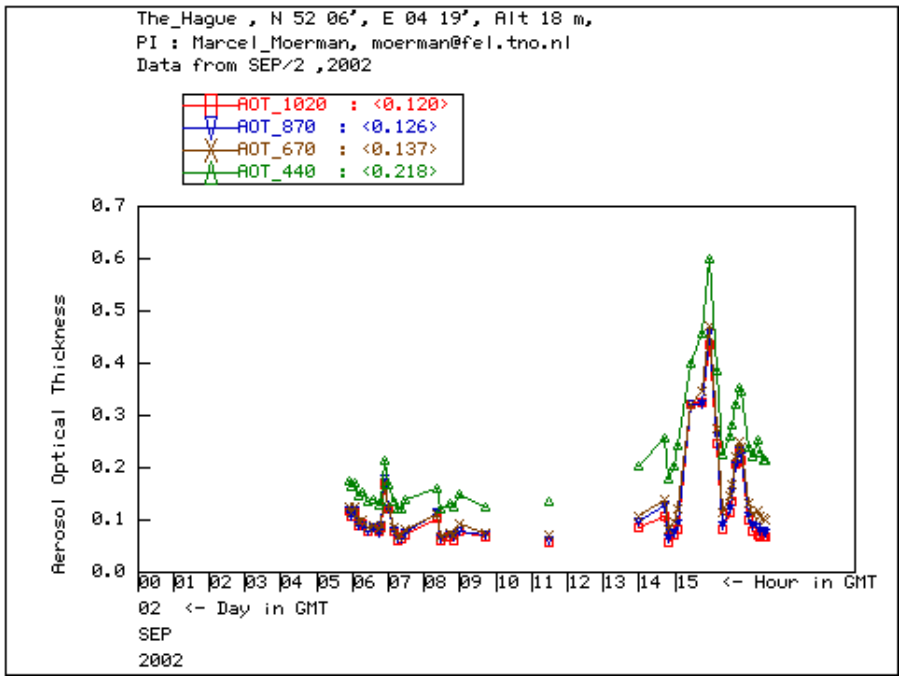

*Figure **Fout! Opmaakprofiel niet gedefinieerd.**.2 AeroNet data (CIMEL) for the 'The Hague' station (data courtesy Marcel Moerman, TNO-FEL).*

The low aerosol content is also supported by the MERIS level 2 aerosol optical thickness product that gives the same value (~0.1). Wind speed data was available very close (less than 10 km) to the match-up station, indicating that a moderate breeze (6 ms^{-1}) was blowing from the East (data courtesy KNMI).

4.4 Results

Of the four stations that were visited on the second of September, two fall within 1 hour of the MERIS overpass (10:29 UTC). Station 1 was sampled at 10:30 and Station 2 was sampled at 11:20 UTC. The corresponding match-up pixels that were identified for the 2 September image are given in Table 4.2 (geometries) and Table 4.3 (flag values). The match-up locations, the CIMEL station and the wind speed station are indicated in a subset of the MERIS image in Figure 4.5.

Both stations are close to the coast, and patterns of suspended sediment are visible within the true colour image. Because the pixels are located in the middle of the MERIS swath, they have near-nadir viewing geometry (camera 3), which might result in medium sunglint (the 'medium_glint' flag was raised). Both pixels also have the case2 flag raised. The in situ concentrations and relevant inherent optical properties that were measured at both match-up stations are presented in Table 4.6 and compared with the

MERIS pixels and a 3x3 pixel box around the match-up pixels to indicate the variance in the MERIS values due to between-pixel natural variability. This between pixel variations must be taken into account because geo referencing is typically performed with an uncertainty of approximately one pixel. For station 1 we compared both in situ concentrations and reflectance, but for station 2 the PCD flags were raised for the concentration products, so we only compared reflectance.

4.4.1 Concentrations

When comparing the in situ measured concentrations, we see that, for station 1, the chlorophyll-a concentration measured in situ (5.8 and 6.4 for the optical method and the spectrophotometric method, respectively) is significantly lower than the MERIS algal pigment index 2 for the nearest neighbour pixel (9.8) and also lower than the minimum found for the 3x3 box surrounding the nearest neighbour pixel (8.3). The TSM concentration measured in situ (4.2 and 3.6 for the optical method and the gravimetric method, respectively) is within 25% of the MERIS total suspended matter product (4.4) and (almost) falls within the minimum and maximum value (3.7 and 6.6) found in the 3x3 pixel box around the nearest neighbour pixel. The yellow substance absorption at 442 nm measured in situ (0.53) is significantly higher than the MERIS yellow substance product (0.20) and falls outside the minimum and maximum value (0.18 and 0.34) found in the 3x3 pixel box around the nearest neighbour pixel.

4.4.2 Reflectance

The comparison of the reflectance is based on the spectra found within the 3x3 box of pixels around the match-up (nearest neighbour) pixel in the MERIS image, and the tri-replicate of reflectance measurements made by the above water radiometry measured from the ship. No conversions were made to correct for the geometry differences between MERIS (near nadir) and the reflectance measured from the ship (40° nadir angle). The reflectance for station 1 and 2 are presented in Figure 4.3 and Figure 4.4, respectively. The three spectra that were measured in situ are presented as three blue lines. The minimum and maximum MERIS reflectance are presented as thin orange lines, the match-up pixel reflectance is presented as a dotted thick orange line and the median of the 3x3 pixel box is presented as a thick orange line. The hyperspectral reflectance data was converted to MERIS bands using the appropriate MERIS spectral response curves.

For both stations there is an overlap between the three blue lines (in situ spectra) and the minimum and maximum values found within the 3x3 pixel box, which means that the MERIS reflectance is consistent with the in situ measured reflectance. For band 1 to 5 the difference between the mean in situ spectrum and the MERIS match-up reflectance is smaller than 0.005, for band 6 to 11 the difference is smaller than 0.001.

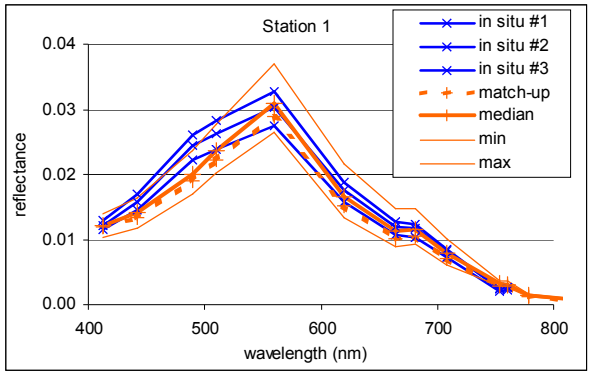

Figure ***Fout! Opmaakprofiel niet gedefinieerd.****..3 Comparison between in situ measured reflectance and MERIS derived reflectance for station 1. The median, minimum and maximum values are calculated over a 3x3 pixel box around the match-up pixel.*

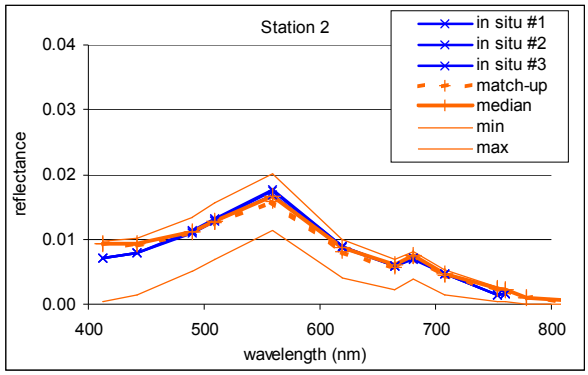

Figure ***Fout! Opmaakprofiel niet gedefinieerd.****..4 Comparison between in situ measured reflectance and MERIS derived reflectance for station 2. The median, minimum and maximum values are calculated over a 3x3 pixel box around the match-up pixel.*

*Figure **Fout! Opmaakprofiel niet gedefinieerd.**.5 Map of match-up stations, CIMEL location, and wind speed station plotted on top of the MERIS image (true colour) of 2 September 2002.*

4.5 Conclusions and Recommendations

For two match-up pixels it was found that the reflectance values and the suspended matter concentrations were consistent with in-situ observations. The algal pigment 2 was significantly higher and the yellow substance absorption was significantly lower than the in situ observations. For band 1 to 5 the difference between the mean in situ spectrum and the MERIS match-up reflectance is smaller than 0.005, for band 6 to 11 the difference is smaller than 0.001.

Only two match-up pixels are presented in this paper, so no statistically sound conclusive remarks can be made about the validation level of MERIS for the geophysical products that were discussed. Combination with other match-up pixels under different atmospheric conditions and for different concentration ranges are necessary to gain more insight in the MERIS validation. On the other hand also more in-depth research is needed to understand the nature of the differences between in situ and MERIS observations.

In future, the following points should be addressed to improve the knowledge on MERIS validation

1. Processing and delivery of more MERIS scenes to provide more match-up stations and to allow a better statistical approach to MERIS validation.
2. Investigate the influence of MERIS degradation on the level-2 geophysical products
3. Have a closer look at the atmospheric correction performance, especially above complex case II waters in the blue part of the spectrum.

4. Investigate full resolution MERIS products to get a better understanding of between and sub pixel variation (NB the full resolution image was not available during the course of this project).
5. Compare MERIS products with historical in situ data to investigate possible systematic biases in the level 2 products
6. Perform vicarious calibration of MERIS with other ocean colour sensors such as SeaWiFS and MODIS.
7. Continue validation-cruises in 2003 to get more potential match-up stations.

4.6 Tables

*Table **Fout! Opmaakprofiel niet gedefinieerd.**.1 Cruise overview for 2002.*

date	status	Date	status
25 March	skipped	29 July	skipped
8 April	joined	5 August	skipped
29 April	skipped	12 August	skipped
6 May	skipped	19 August	skipped
27 May	skipped	26 August	skipped
3 June	joined	2 September	joined
24 June	skipped	16 September	skipped
1 July	skipped		

*Table **Fout! Opmaakprofiel niet gedefinieerd.**.2 Overview of the viewing geometry (degrees) and location (DMS) of the match-up pixels.*

	Lat:	Lon:	sun zenith	sun azimuth	view zenith	view azimuth
STATION 1	52º10'32" N	4º15'58" E	47	155	4	287
STATION 2	52º14'21" N	4º16'55" E	47	155	4	287

*Table **Fout! Opmaakprofiel niet gedefinieerd.**.3 Overview of relevant flag values for the match-up pixels.*

	reflec	alg. pig. 1	ys, spm	alg. Pig. 2	ABSOA_CONT	ABSOA_DUST	CASE2_S	CASE2_Y	MEDIUM_GLINT	HIGH_GLINT
STATION 1	FALSE	TRUE	FALSE	FALSE	FALSE	TRUE	TRUE	FALSE	TRUE	FALSE
STATION 2	FALSE	TRUE	TRUE	TRUE	FALSE	TRUE	TRUE	FALSE	TRUE	FALSE

*Table **Fout! Opmaakprofiel niet gedefinieerd.**.4 Statistics for relevant and valid (no PCD flag raised) MERIS geophysical products extracted from the MERIS image for station 1. The mean, median, min and max were calculated over a 3x3 pixel box around the nearest neighbor pixel.*

Product	nearest neighbor	mean	median	min	max
reflec_1	0.012	0.012	0.012	0.010	0.014
reflec_2	0.013	0.014	0.014	0.012	0.016
reflec_3	0.019	0.020	0.020	0.017	0.024
reflec_4	0.022	0.024	0.024	0.020	0.028
reflec_5	0.029	0.031	0.031	0.026	0.037
reflec_6	0.015	0.017	0.017	0.013	0.022
reflec_7	0.010	0.012	0.011	0.009	0.015
reflec_8	0.011	0.012	0.011	0.009	0.015
reflec_9	0.007	0.008	0.008	0.006	0.010
reflec_10	0.003	0.003	0.003	0.003	0.004
reflec_11	0.003	0.003	0.003	0.003	0.004
reflec_12	0.001	0.001	0.001	0.001	0.002
reflec_13	0.000	0.000	0.000	0.000	0.000
algal_2	9.8	9.4	9.3	8.3	10.4
yellow_subs	0.20	0.254	0.256	0.177	0.335
total_susp	4.4	5.1	4.9	3.7	6.6

*Table **Fout! Opmaakprofiel niet gedefinieerd.**.5 Statistics for relevant and valid (no PCD flag raised) MERIS geophysical products extracted from the MERIS image for station 2. The mean, median, min and max were calculated over a 3x3 pixel box around the nearest neighbor pixel.*

Product	nearest neighbor	mean	median	min	max
reflec_1	0.009	0.007	0.009	0.001	0.010
reflec_2	0.009	0.008	0.009	0.001	0.010
reflec_3	0.011	0.010	0.011	0.005	0.013
reflec_4	0.013	0.012	0.013	0.007	0.016
reflec_5	0.016	0.016	0.017	0.011	0.020
reflec_6	0.008	0.008	0.009	0.004	0.010
reflec_7	0.006	0.005	0.006	0.002	0.007
reflec_8	0.007	0.007	0.008	0.004	0.008
reflec_9	0.004	0.004	0.005	0.001	0.005
reflec_10	0.002	0.002	0.002	0.000	0.003
reflec_11	0.002	0.002	0.002	0.000	0.002
reflec_12	0.001	0.001	0.001	0.000	0.001
reflec_13	0.000	0.000	0.000	0.000	0.000

*Table **Fout! Opmaakprofiel niet gedefinieerd.**.6 In situ parameters for station 1 and 2.*

Parameter	Station 1	Station 2
chl-a, spectrophotometric (mg m^{-3})	6.4	8.2
phytoplankton pigment absorption at 442 nm (m^{-1})	0.142	0.209
chl-a[1] calculated from pigment absorption (mg m^{-3})	5.8	7.9
total suspended matter (g m^{-3})	3.6	3.7
particle scattering (m^{-1})	3.1	2.0
total suspended matter[2] (g m^{-3})	4.2	2.7
yellow substance absorption at 442 nm (m^{-1})	0.53	0.54

[1] using a conversion factor of $chl = 26.212 \cdot a_{pig}(442nm)^{0.77135}$.

[2] using a conversion factor of $TSM = 1.73 \cdot b_p$.

5. Processed MERIS and CASI observations

The validation campaign in summer 2002, as described in the previous chapter, included the fly-over with the EPS-A airborne scanner in the Coast Guard plane. Due to major problems with instrument itself and logistic problems the EPS-A observations of the North Sea waters near the Dutch coast could not be scheduled for the summer of 2001 and 2002. Instead the Survey Department (MD) has hired the CASI instrument from the Freie Universität Berlin. In this chapter the observations made by the CASI instrument, the atmospheric correction and the derived water quality maps are described. The observations are compared to MERIS products obtained one day before. Both instruments have similar band settings (see Figure 5.1).

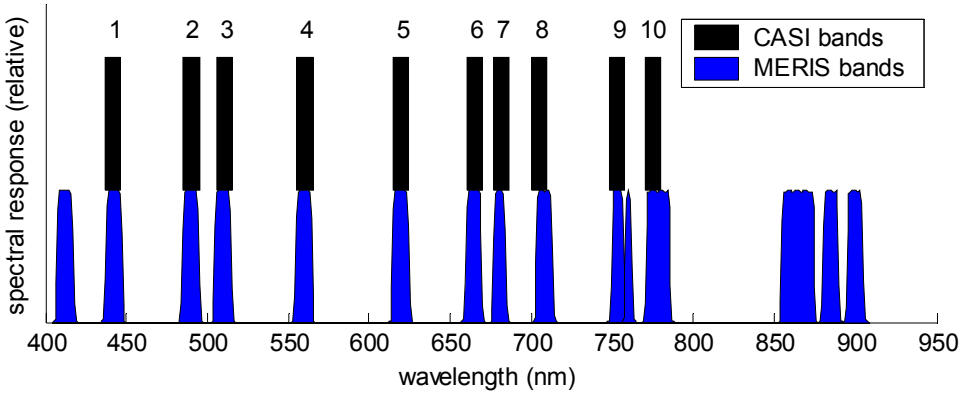

*Figure **Fout! Opmaakprofiel niet gedefinieerd.**.1 Spectral response curves from MERIS and CASI.*

Note that the relationship between the phytoplankton absorption and the chlorophyll concentration is determined near the maximum in the specific phytoplankton absorption at 672 (MERIS band setting) or 665 (for this CASI band setting). This factor is not constant, but is different for each type of algae and the physiological state of the algae. Effectively, it depends on the phytoplankton pigment composition, packaging effect and photo adaptation of the pigments. For the processing of the MERIS and CASI images we therefore sought for measurements that best represent the area and season of image capture (2/3 September 2003).

5.1 Processing of a MERIS image with regional algorithms

The prototype MERIS processor was tested using the -reduced resolution- MERIS image of 2 September 2002, that was nearly coincident with the CASI overpass. Unluckily, the flight lines of the CASI instrument were positioned over the mouth of the Western Scheldt estuary, whereas the in situ reflectance measurements, measurements of inherent optical properties and concentrations were taken on board the RV Mitra, that was located near RWS station Noordwijk10. This station is approximately 10 km off the coast, near

the city of Noordwijk. Therefore the algorithms to be used over the Western Scheldt could not be regionally calibrated with the measured in situ specific inherent optical properties. Comparison of the standard MERIS product with the measured reflectance and concentrations at station Noordwijk10 was done within the validation chapter 4.

This chapter focuses on the Western Scheldt region. Two algorithms were tested, one for the chlorophyll-a concentration and one for the total suspended sediment concentration. Both algorithms were applied to the level 2 MERIS image using the prototype MERIS processor, described in Appendix I.

Chlorophyll-a concentration

The algorithm used to retrieve the chlorophyll-a concentration is based on the work published by Gons (1999) and uses the ratio of two red bands, one with high chlorophyll-a absorption (at 672 nm), and one with low chlorophyll-a absorption (at 704 nm). A near-infrared band (at 776 nm) is used to estimate background particle scattering. The bands that were used in the application for MERIS are listed in the following table.

*Table **Fout! Opmaakprofiel niet gedefinieerd.**.1 Applied MERIS bands and central wavelengths.*

Original wavelength	MERIS wavelength	MERIS band
672	664	7
704	708	9
776	778	12

The coefficients used in the algorithm, i.e. pure water absorption in the three bands and the specific chlorophyll absorption at 672, where adapted according to the slightly different spectral position of the MERIS bands compared to the original algorithm (Table 5.2).

*Table **Fout! Opmaakprofiel niet gedefinieerd.**.2 Applied settings and values for MERIS bands.*

parameter	value
pure water absorption at 664 nm	0.40 m^{-1}
pure water absorption at 708 nm	0.71 m^{-1}
pure water absorption at 778 nm	2.35 m^{-1}
specific phytoplankton absorption at 664 nm	0.0169 $mg^{-1}m^2$

For the calculation of the band ratio, it was assumed that the effective upward and downward transmittance through the air-water interface was wavelength-independent and thus does not influence the ratio. For the NIR band an effective air-water interface correction factor of 0.54 was used, typical for the small viewing zenith angles (viewing zenith angles over the Western Scheldt area are between 0 and 4°). The f/Q ratio was retained from the original algorithm ($f = 0.082Q$).

The image was flagged on a pixel-wise basis using the cloud and land flag and the confidence flag (PCD) for the MERIS level 2 reflectance product. Flagged pixels were printed black. The result for of the chlorophyll-a concentration is presented in figure 5.2. Note that this image is at reduced resolution. In full-resolution, the spatial pattern in the Western Scheldt estuary will be better resolved.

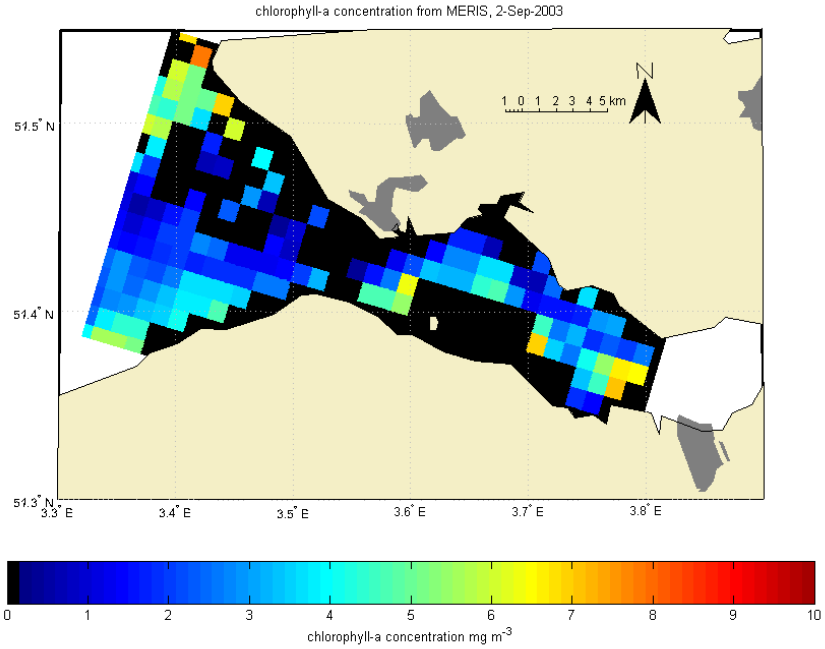

Figure ***Fout! Opmaakprofiel niet gedefinieerd.****..2 Chlorophyll-a concentration estimated from MERIS.*

For the calculation of the suspended matter concentration, the one-band algorithm used in the POWERS-II project was used (Van der Woerd et al., 1999). This algorithm was also used for the series of atlases of suspended matter in the North Sea, based on SeaWiFS images. The coefficients were adapted because MERIS has a different band setting than SeaWiFS (SeaWiFS: 555 nm; MERIS 559 nm), the same f/Q was used as in the chlorophyll algorithm. The one-band algorithm is in fact a one band analytical inversion with fixed values for chlorophyll concentration and g_{440} (5 mg m^{-3} and 0.34 m^{-1}, respectively). After rewriting this results in the following formulation:

$$TSM = \frac{n_1 R_{559} + n_2}{d_1 + d_2 R_{559}} \qquad \textbf{(Fout! Opmaakprofiel niet gedefinieerd.}..1)$$

Where R_{559} is the subsurface irradiance reflectance in band 5, and n_1, n_2, d_1 and d_2 are coefficients with values listed in the following table.

*Table **Fout! Opmaakprofiel niet gedefinieerd.**.3 Parameters of equation 5.1.*

coefficient	value
n_1	0.1717
n_2	-2.6372e-004
d_1	0.0054
d_2	-0.0251

The image was flagged on a pixel-wise basis using the cloud and land flag and the confidence flag (PCD) for the MERIS level-2 reflectance product. Flagged pixels were printed black. The result is presented in Figure 5.3.

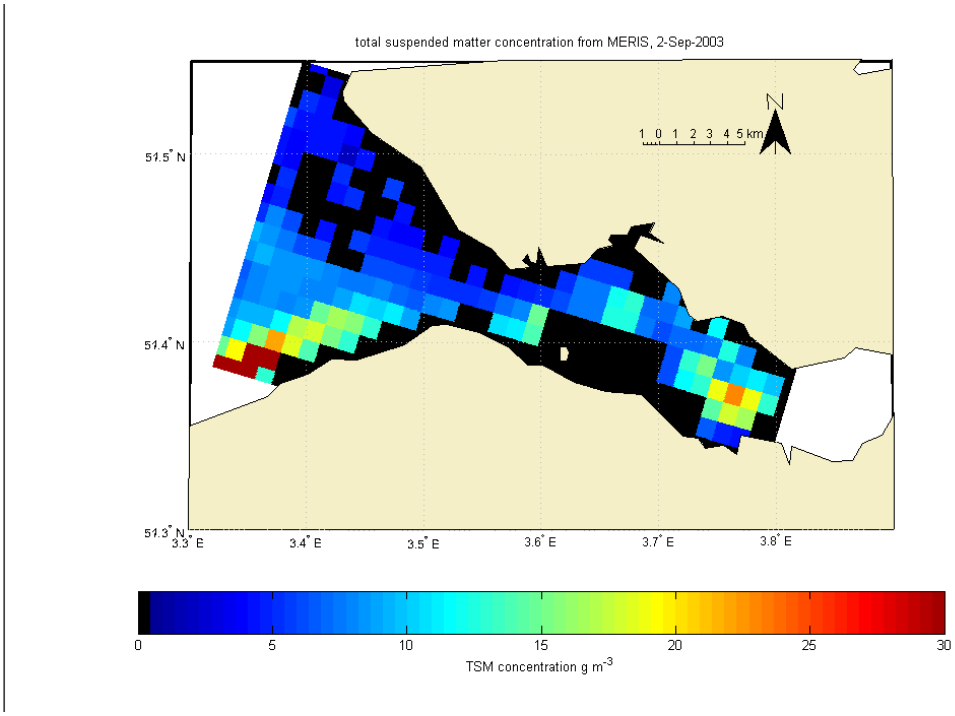

*Figure **Fout! Opmaakprofiel niet gedefinieerd.**.3 Total suspended matter concentration estimated from MERIS.*

5.2 Processing of CASI imagery

In preparation of MERIS processing, a CASI instrument was flown over the Western Scheldt estuary on 3 September 2002. Three flight lines were recorded, of which the location is indicated in Figure 5.4. Flight line 1 was recorded from 10:31 - 10:35, Flight line 2 was recorded from 10:49 - 10:56 and line 3 was recorded from 10:57 - 11:05, all in UTC time zone. The azimuth angle of the flight lines was approximately 109° (relative to North). The predicted solar elevation and solar azimuth angle for Tuesday 3 September 2002 as a function of the flight times are given in Table 5.4.

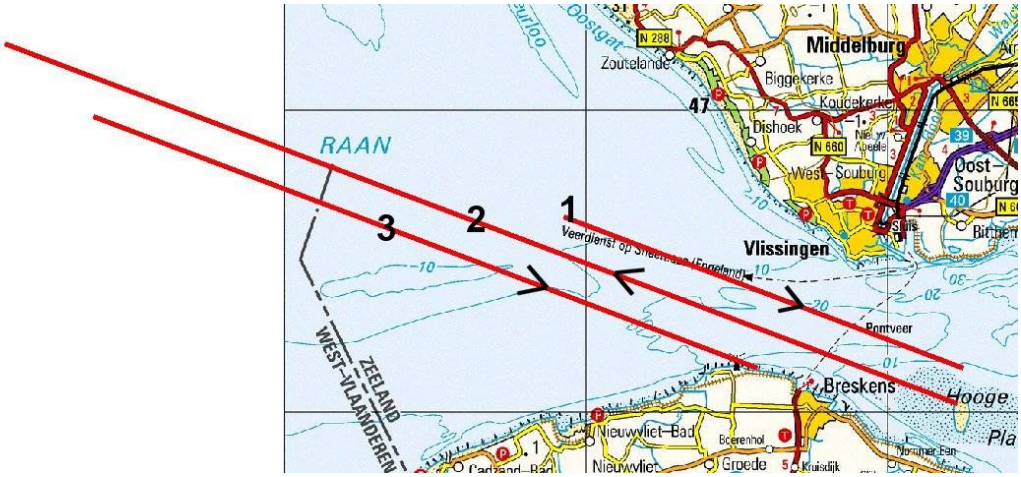

Figure ***Fout! Opmaakprofiel niet gedefinieerd.****..4 Three CASI flight lines.*

Table ***Fout! Opmaakprofiel niet gedefinieerd.****..4 Predicted Solar geometry on September 3, 2002.*

CASI flightline	time (UTC)	Solar elevation	Solar azimuth
1	10:33	44	155
2	10:52	45	161
3	11:01	45	164

After radiometric correction by the CASI operator, the images were atmospherically corrected by the Survey Department, after which they were copied to the Institute for Environmental Studies on CD-ROM media.

The metadata about conditions, flight path and band-settings were studied, and the img-files were opened in ERDAS Imagine. Upon first view it appeared that the data comprises sun glint, and a blue disturbance along the edge of the strip.

This sun glint is a commonly encountered problem in imagery recorded by airplanes. This phenomena occurs when the line of sight of the instrument and the direction sun allow direct scattering (glint) of solar radiance into the field of view of the sensor. Because the scan direction of the CASI instrument is perpendicular to its flight direction, the angle between the solar azimuth and the flight direction azimuth should be minimal (i.e. 0°). A worst case arises when the solar azimuth is perpendicular to the flight direction azimuth (i.e. 90°). For this particular case the azimuth difference was (for flight line 2) 52°, resulting in considerable sun glint in the images, especially at the South side of the image strips. It is (nearly) impossible to correct for sun glint, because the radiance levels arising from sun glint are typically much higher than the water-leaving radiance. Moreover, with meter-sized pixels the signal is highly variable because of the wind-driven variation in wave slopes.

Therefore it was decided that these pixels had to be filtered out by constructing a mask using bands in the near-infrared reach. First of all, however, the data were classified with the chlorophyll and TSM algorithms using ERDAS Imagine option ‘Modeler’. For this,

flight line 2 was chosen (Figure 1). This strip was atmospherically corrected at the Survey Department with estimated horizontal visibility settings of 35.0 km. The length of strip is approximately 33.7 kilometres and the width of strip is approximately 2.6 kilometres (assuming square pixels).

As mentioned before this image has visible sun glint and blue (stray light?) disturbance at the same side of the swath so that only one side is (visibly) disturbed. The influence of sun glint on the other side of the swath is difficult to assess, but might be of considerable importance for later water quality retrievals. The sight parameter setting of 35 km gave a minimum amount of negative radiances as compared to lower visibility settings. A true-colour composite is shown in figure 5.5.

Chlorophyll-a concentration

The Gons algorithm (Gons, 1999) was used for chlorophyll retrieval:

$$CHL-a=\left(\frac{R(0^-)_{704}}{R(0^-)_{672}}\left(a_{w,704}+b_{b776}\right)-a_{w672}-b_b\right)/\left(a^*_{TCHL,672}\right)$$

(**Fout! Opmaakprofiel niet gedefinieerd.**.2)

The following input values were used:

- R672, R704, R776, Subsurface irradiance reflectance at 672, 704 and 776 nm, CASI bands 6, 8, and 10, respectively
- Bb776=2.7097*R776/(Q*0.082-R776);
- Q, a Q-factor used by Gons (1999), Q = 3.75 (value also used by the Survey Department (Meetkundige Dienst, 2003))

Bands 6, 8 and 10 were extracted in ERDAS Imagine with Interpreter, Utilities, Subset. They were extracted in Float Double format in order to prevent any problems that might otherwise occur during map calculations. Details for the map calculations can be found in Appendix II.

TSM concentration

The POWERS algorithm (Van der Woerd et al., 2000)was used for TSM Retrieval: see the equations above. Note however, that R_{555}, Subsurface irradiance reflectance at 555 nm, CASI bands 4 was used, instead of the 559 values.

Details for the map calculations can be found in Appendix II.

5.2.2 Masking

The CASI images have to be corrected for scatter and the blue stripe. To do this a mask was made based on the principle that clear water is truly black in the near infrared reach, and coastal water with sediments or algae also should not have too high values. Scatter and other disturbances will give high values. After visual inspection of band 10 the boundary was defined as < than 0.03. Modeller was used to create the mask. Details for the map calculations can be found in Appendix II.

To make the outcome more visually attractive the map could be enhanced by post-processing through interpolation (with, e.g., GIS analysis, Clump), but here we would like to report true values only.

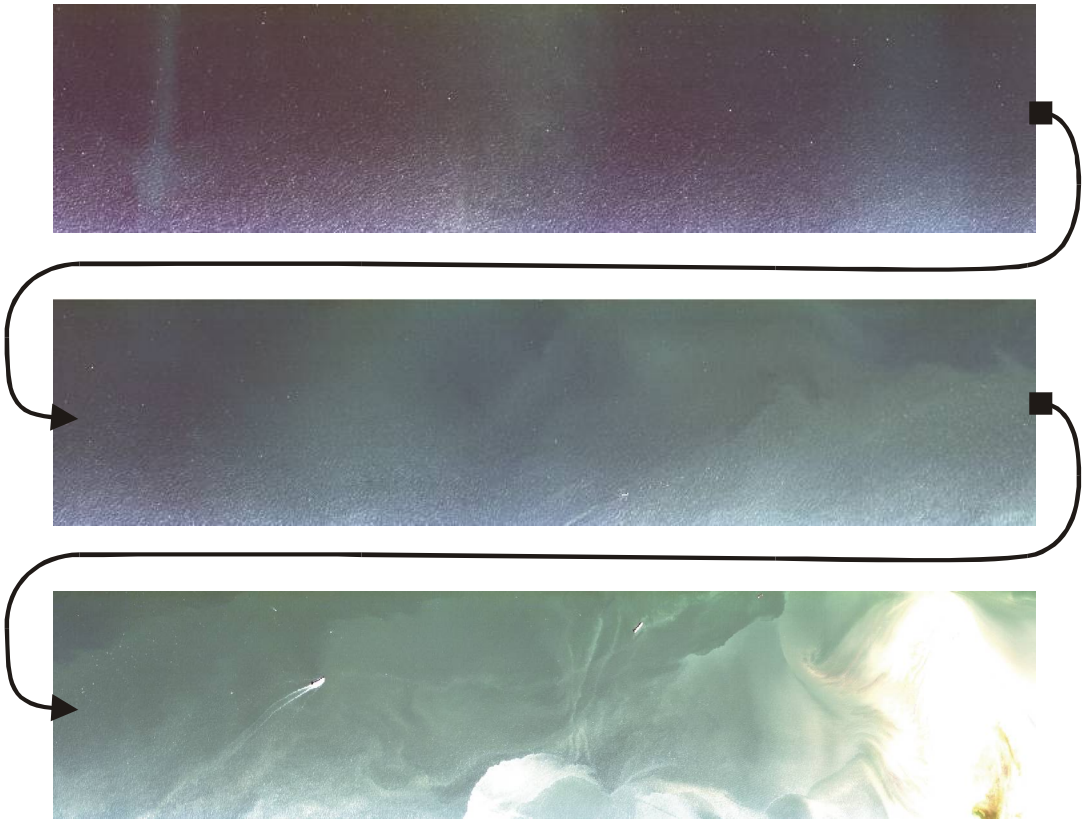

*Figure **Fout! Opmaakprofiel niet gedefinieerd.**.5 True colour composite image of the input file (from band 5,4 and 2).*

5.2.3 Results

All produced output was saved to disk in native ERDAS image format, so that it remains available for any further processing. For visualisation purposes, the imagery was transferred to Matlab where basic GIS maps were created using the mapping toolbox. The result for the total suspended matter concentration is plotted in Figure 5.6.

The observed sediment patterns are comparable to the values found in the processed MERIS image. TSM concentrations in the open North Sea are generally smaller than 5 gm-3, whereas the concentration towards the mouth of the estuary rapidly increase. It is difficult to assert how severely the elevated concentrations at the South of the image strip are affected by sun glint.

The retrieved chlorophyll-a concentrations from the CASI image are dissatisfactory and are not shown here. The values were unreasonably high and well above the expected

values for the time and location of the image (expected values: open North Sea: smaller than five, Western Scheldt: between 5 and 10 mg m^{-3}).

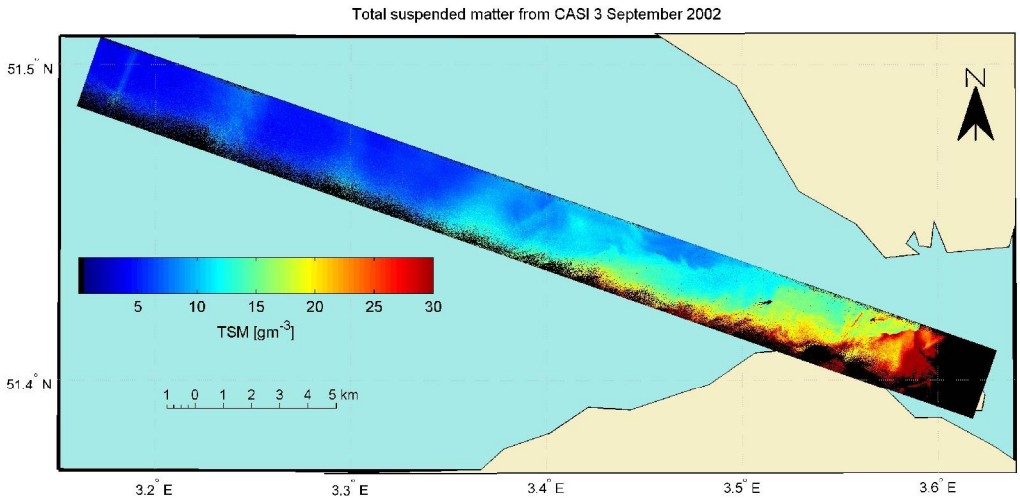

*Figure **Fout! Opmaakprofiel niet gedefinieerd.**.6 Derived TSM concentrations from the CASI image of September 3, 2002. Sun glint flagged pixels are plotted black. The geometric correction is only indicative. Land is plotted yellow, not covered water is plotted light blue.*

The chlorophyll-a product might be improved by considering:

1. Re-evaluating atmospheric correction. Especially the reflectance in the NIR was found to be significantly too large, which might be an indication for sub-optimal atmospheric correction performance.
2. Comparison of MERIS reflectance with CASI reflectance to see where the main differences are and how those differences influence the retrieved chlorophyll-a concentration.

References

Dekker, A.G., Brando, V.E., Anstee, J.M., Pinnel, N., Kutser, T., Hoogenboom, E.J., Peters, S., Pasterkamp, R., Vos, R., Olbert C. & Malthus, T.J.M. (2001). Imaging spectrometry of Water. In Meer, F.D. van der & Jong, S.M. de (Eds.), *Imaging Spectrometry*. Dordrecht, Kluwer.

Doerffer, R., (2002). *Protocols for the Validation of MERIS Water Products*. PO-TN-MEL-GS-0043, GKSS, Germany, 42 pp.

Fargion, G.S. & Mueller, J.L. (2000). *Ocean Optics Protocols For Satellite Ocean Color Sensor Validation*, Revision 2, NASA/TM-2000-209966, Goddard Space Flight Space Center, Greenbelt, Maryland, USA, 184 pp.

Gons, H.J. (1999). Optical teledetection of chlorophyll-a in turbid waters. *Environmental Science Technology*, 33 (7), 1127-1132.

Gordon, H.R., Brown, O.B. & Jacobs, M.M. (1975). Computed relationships between the inherent and apparent optical properties of a flat homogeneous ocean. *Appl. Opt.,* 14 (2), 417-427.

Hoge, F.E & Lyon, P.E. (1996). Satellite retrieval of inherent optical properties by linear matrix inversion of oceanic radiance models. *J. Geophysical Res.-Oceans*, 101 (C7), 16631 – 16648.

McClain, C.R., (2000). *SeaWiFS postlaunch calibration and validation overview*, NASA Tech. Memo. 2000-206892 Vol. 9, NASA Goddard Space Flight Center, Greenbelt, Maryland, USA, 12 pp.

Meetkundige Dienst (2003). *CASI-opnamen Noordzee*: 3 september 2002. (2 CD's).

Mobley, C.D., (1999). Estimation of the remote-sensing reflectance from above-surface measurements. *Appl. Opt.,* 38 (36), 7442-7455.

Mueller, J.L., R.W.Austin, (2000). *Ocean Optics Protocols for SeaWiFS Validation*, NASA Tech. Memo. 2000-104566 Vol. 25, NASA Goddard Space Flight Center, Greenbelt, Maryland, USA, 39 pp.

NEN 6520, (1981). Water: Spectrophotometric determination of chlorophyll a content. *Nederlandse Norm.*

Peters, S.W.M., Vos, R.J., Hoogenboom, E.J., Hakvoort, H., Wernand, M., Woerd, H.J. van der, Rijkeboer, M. & Pasterkamp, R. (2001). *MERIS for water quality monitoring in the Belgian-Dutch-German coastal zone*. BCRS-report, USP-2 01-25, 122 pp.

Sørensen, K., (2002). *Comparisons of Chlorophyll HPLC, Spectrophotometric Measurements.* In Sawaya-Lacoste, H. (Ed.), Proceedings of the Envisat Calibration review, 9-12-2002, ESA Publications division, in press.

Tilstone, G. H., Moore1, G. F. , Sørensen, K. Doerffer, R. Røttgers, R., Ruddick, K. G. Pasterkamp, R. & Jørgensen, P.V. (2002). *REVAMP Protocols Document,* Plymouth Marine Laboratories, Plymouth, 44 pp.

Trüper, H.G. & Yentsch, C.M. (1967). Use of glass fiber filters for the rapid preparation of in vivo absorption spectra of photosynthetic bacteria. *J. Bact.,* 94, 1255-1256.

Van der Woerd, H., J.H.M. Hakvoort, H.J. Hoogenboom, Omtzigt N., R. Pasterkamp, S.W.M. Peters, K.G. Ruddick, de Valk C., R.J. Vos, (2000). *Towards an operational monitoring system for turbid waters*, O-00/16, IVM\VU Amsterdam, 62 pp.

Appendix I. MERIS prototype processing infrastructure

The MERIS L1, L2 and L3 measurement datasets (MDS) will be delivered in a special ESA format. Because this is a new format, regular image processing software will not be able to handle these product formats. However, several tools were developed by ESA to read, process and analyse the MERIS data products (http://envisat.esa.int/services/tools_table.html)

The MERIS/(A)ATSR Toolbox (MATBX)

The MERIS/(A)ATSR Toolbox (MATBX) is a collection of executable tools and an application programming interface (API) which has been developed to facilitate the utilisation, viewing and processing of ESA MERIS, (A)ATSR and ASAR data. The purpose of the MATBX is not to duplicate existing commercial packages, but to complement them with functions dedicated to the handling of ENVISAT MERIS and AATSR products.

The main components of the MATBX are

- VISAT - A visualization, analyzing and processing software, entirely written in Java
- A set of scientific tools running either from the command line or invoked by VISAT, also entirely written in Java.
- The MATBX Java API provides software frameworks and helpers for application development and new extension modules
- ENVISAT MERIS/AATSR Product Access API for ANSI C allowing reading access to these data products using a simple programming model.

The development of the MATBX software is targeted as an open source project and comes with full source code. The MATBX version 1.0 will be released in December 2002.

EnviView

EnviView is a free application that allows Envisat data users to open any Envisat data file and examine its contents. It provides simple visualisation capabilities, and allows data to be exported to HDF for use in other software packages.

Both VISAT and Enviview are intended to display data and do manual operations, but are less suited to do automatic processing of images or do more complex operations like the pixel or transect extraction, which is essential for validation activities. Within workpackage 3 of the MERIMON project the MERIS processing architecture for regional products generation (MEPARP) was developed. The principal conditions for the MEPARP are

1. Ability to read MERIS Reduced Resolution Geophysical Products (MER_RR__2P)
2. Ability to deal with custom-made regional algorithms
3. Ability to extract pixels or transects, given the geophysical coordinates.

The MERIS software provides tools or interfaces to extract raw data from the MERIS products. These raw data can than be processed by other scientific software packages. ENVIVIEW includes a tool called PDS2HDF, which allows the user to export MERIS measurement datasets to the HDF4 data standard, which is widely used in the scientific

community (e.g. the current SeaWiFS processor at the IVM is based on the HDF4 standard). The MATBX toolbox allows the export of MERIS products to the HDF5 standard and provides a JAVI Application Program Interface and a C Application Program Interface for direct access to the MATBX tools and classes.

Because these tools are already available and are constantly maintained, the MEPARP relies on these tools for import and export of datasets. The MEPARP is divided into two parts.

1. A Matlab function that performs the bookkeeping of the processing and that manages the input and output of data products. This function also includes some additional general tools, of which the main tool is the pixel/transect extractor.
2. Specific algorithm plug-ins that define specific (regional) algorithms. Algorithms are defined here in a very broad scope, and can be any Matlab function that requires HDF or ENVISAT data.

The philosophy behind this architecture is that a specific algorithm plug-in does not have to worry about input and output of data, because the calculation part of the algorithm is automatically fed with the correct datasets. The definitions of theses datasets were first provided to the processor by the input/output definition sub function of the algorithm. A dataset is primarily described by the dataset type and the dataset name. At the time of writing the processor can handle the following type of datasets (other dataset definitions can be added later, such as HDF5, ASCII, binary, etc.).

*Table **Fout! Opmaakprofiel niet gedefinieerd.**.1 Datasets currently supported by the MEPARP.*

Dataset Identifier (dataset type)	Description
Scientific Data Set	HDF4 Scientific dataset
Vdata set	HDF4 V data set (table)
MDS	ENVISAT Measurement dataset
TiePointGrid	ENVISAT Tie Point Grid

Because the algorithms do not include code for import and export of data, simple algorithms will only take a few lines of Matlab code and can easily be adapted or updated. The MEPARP architecture is schematically presented in the following graph

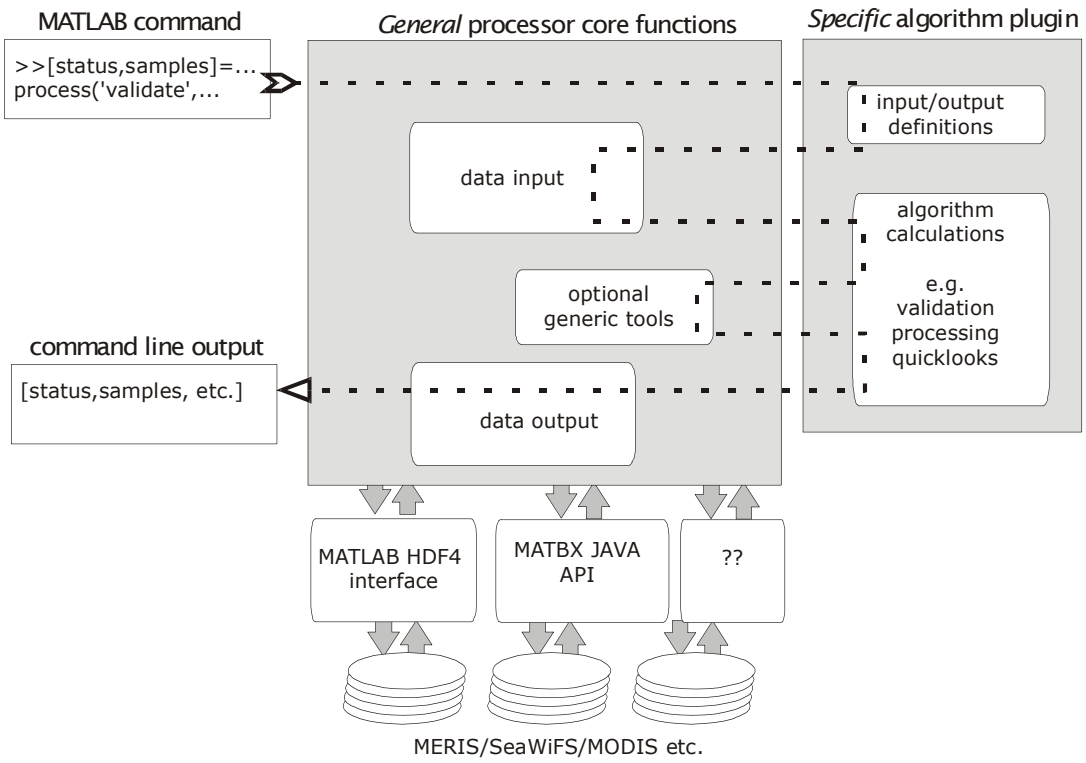

Note that the IVM MERIS prototype-processing infrastructure does not include a graphical user interface but can only be called from the Matlab command line. The processor is compatible with and was tested under Matlab 6.5 (R13). The following algorithms were available at the time of writing of this document

Algorithm plug-in identifier	Algorithm description
Product generators	
P_PMNS_MERIS_CHL_1	PMNS chlorophyll MERIS algorithm
P_PMNS_MERIS_TSM_1	PMNS TSM MERIS algorithm
P_POWERS_SEAWIFS_TSM_1	POWRS TSM SeaWiFS algorithm
Quick look generators	
QL_MERIS_2P_1[a]	Quicklook of MERIS Reduced Resolution Geophysical Product
QL_MERIS_1P_1[a]	True colour quicklook of MERIS Reduced Resolution Geolocated and Calibrated TOA Radiance
Pixel extractors (validation)	
VD_MERIS_2P_2	Extract pixels/transects from MERIS level 2 product
VD_MODIS_OCL2_2	Extract pixels/transects from MODIS Ocean Colour L2 product
VD_SeaWiFS_TSM_1	Extracts values from SeaWiFS TSM (IVM) product

[a] requires Matlab mapping toolbox.

Appendix II. Implementation of the used algorithms in ERDAS imagine

Chlorophyll-a concentration

Map calculations were performed in ERDAS Imagine Modeller. First, Bb776 was calculated (Figure II.1a). Then the nominator of the chlorophyll algorithm was calculated (Figure II.1b), and subsequently the chlorophyll maps were calculated (Figure II.1c and II.1d).

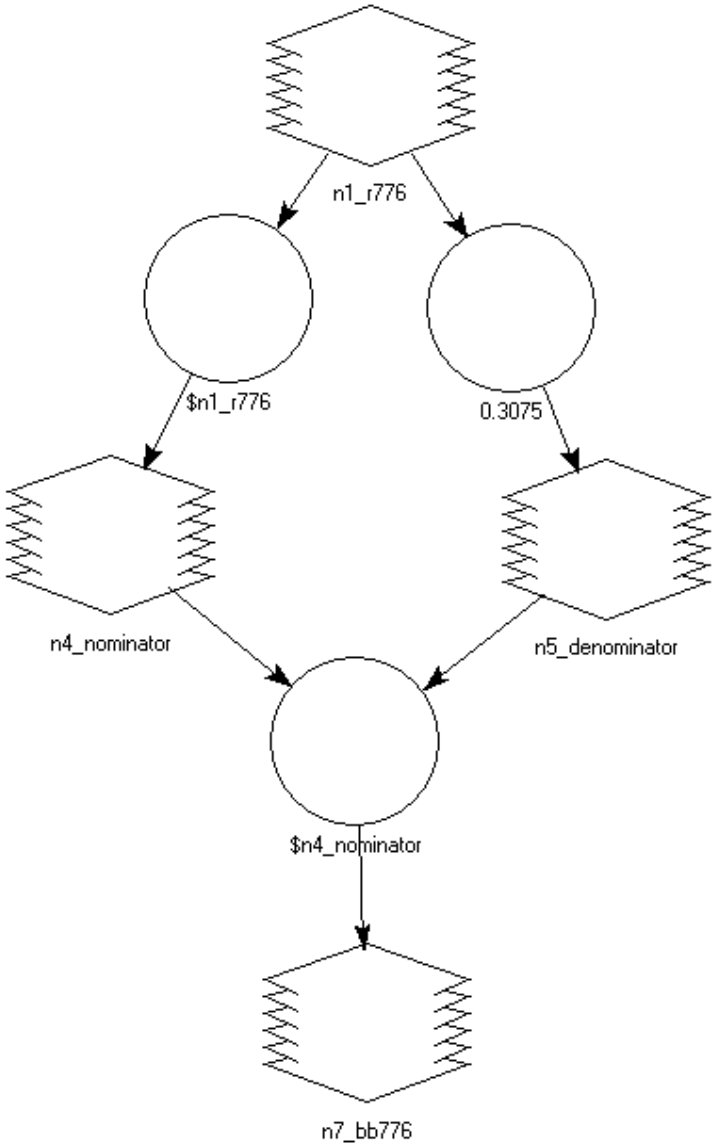

*Figure **Fout! Opmaakprofiel niet gedefinieerd.**.1a Calculation of Bb776.*

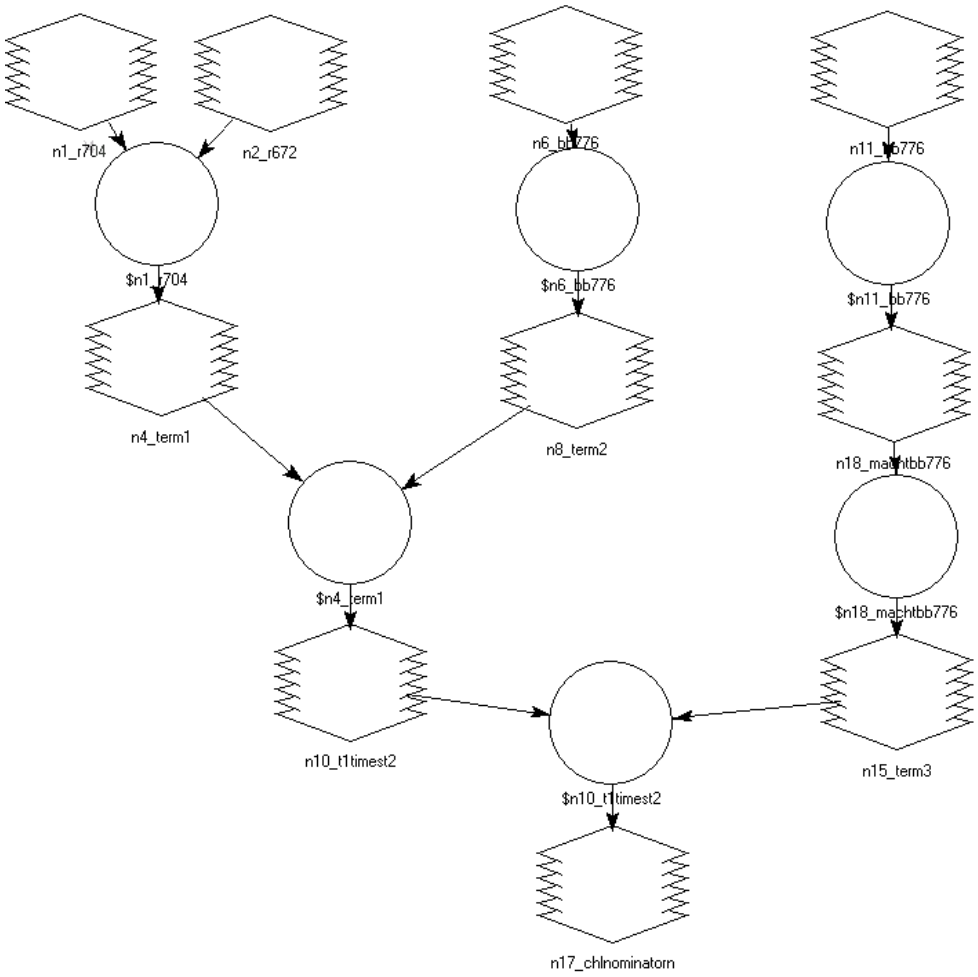

*Figure **Fout! Opmaakprofiel niet gedefinieerd.**.1b Calculation of the nominator of the chlorophyll algorithms.*

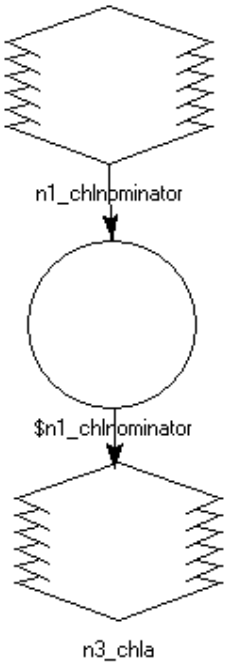

Figure ***Fout! Opmaakprofiel niet gedefinieerd.****.1c Calculation of chlorophyll-a.*

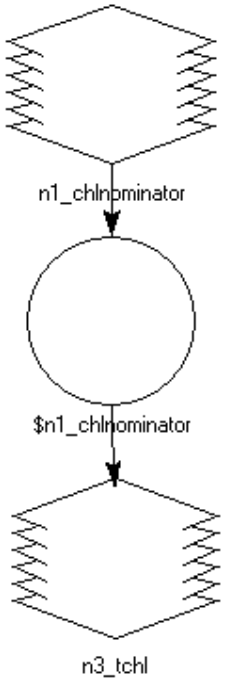

*Figure **Fout! Opmaakprofiel niet gedefinieerd.**.1d Calculation of total chlorophyll.*

Figure II.1 Model for processing CASI bands in order to determine chlorophyll. Because the algorithm is quite complex for Modeler, this was performed in several steps consisting of: (a) Calculation of Bb776, (b) Calculation of the nominator of the chlorophyll algorithms, (c). Calculation of chlorophyll-a, and (d). Calculation of total chlorophyll.

Total suspended matter concentration

In ERDAS Imagine first band 4 was extracted with Interpreter, Utilities, Subset. Then map calculation was performed in Modeller. Figure II.2 shows the elaboration in Modeler, Appendix 2 provides the program in text format.

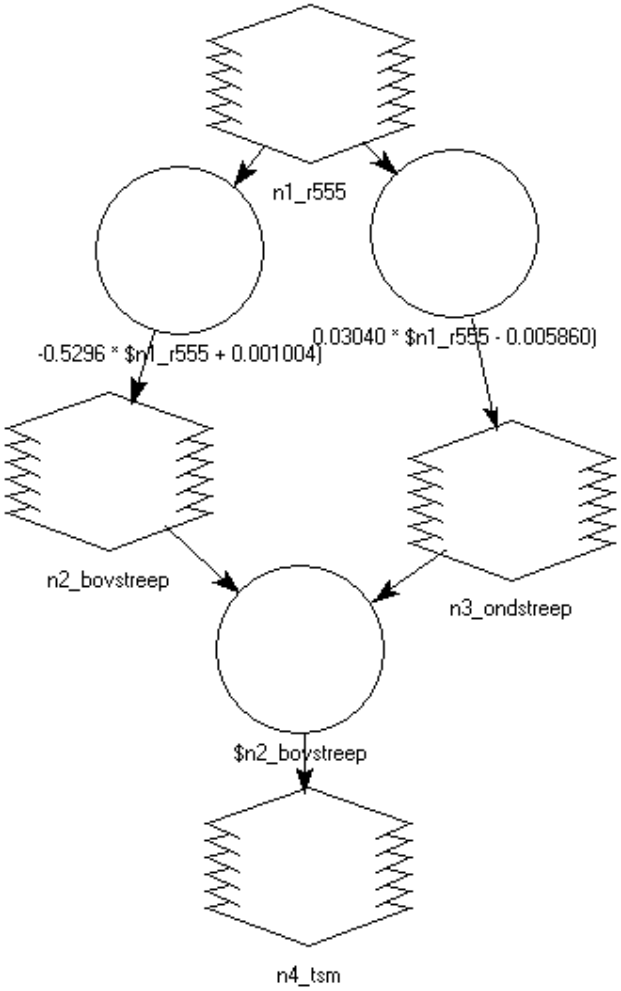

Figure II.2 Model for processing CASI bands in order to determine TSM. The input is R555 (band 4). First the nominator and denominator terms are determined. Then the results are divided. The output is a TSM map.

Masking

Modeller was used to create the mask. (Figure II.3a) and to multiply the mask with Chl-a (Figure II.3b).

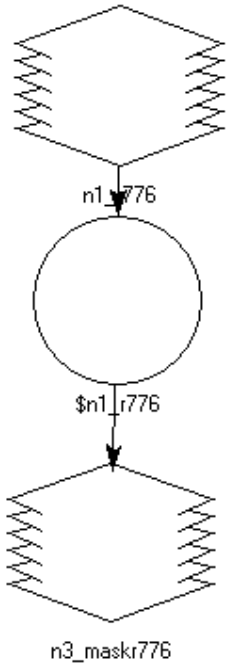

Figure II.3a Creating the mask.

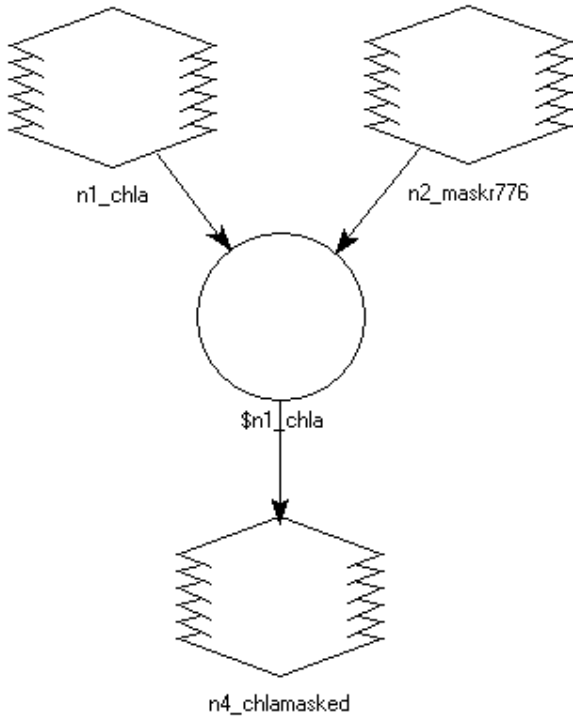

Figure II.3b Model used for masking the Chl-a. To mask TCHL and TSM, the input map on the upper right was substituted by TCHL.img and TSM.img, respectively.